

# Continuum-statistical dynamics of colloidal suspensions under kinematic reversibility

Jerome Burelbach<sup>1</sup>

<sup>1</sup>International School Michel Lucius, 157 avenue Pasteur, 2311 Luxembourg, Luxembourg

May 5, 2026

## Abstract

We present a linear response theory that establishes the continuum-mechanical origin of Onsager reciprocity in colloidal motion. By decoupling hydrostatic and hydrodynamic stress, we show that Onsager reciprocal relations emerge from the Lorentz reciprocal theorem under kinematic reversibility, based on the auxiliary flow problem of colloidal sedimentation. Our framework applies to suspensions containing multiple species of microparticles and derives all non-equilibrium contributions to colloidal diffusion from a single application of the Lorentz reciprocal theorem, irrespective of whether a slip or no-slip hydrodynamic boundary condition is imposed at the colloidal surface. Furthermore, a boundary layer treatment is only assumed for microswimming, while the thermodynamic forces giving rise to phoretic motion are fully resolved beyond the boundary layer approximation. For the diffusiophoretic motion arising from volume exclusion of a solute, our results predict that a colloid is drawn towards regions of higher solute concentration, except when the excluded volume layer around it becomes comparable to its radius. Owing to its linear structure, the framework also enables numerical determination of transport coefficients in dense suspensions without explicitly resolving the underlying microhydrodynamics.

## 1 Introduction

Continuum mechanics describes a multicomponent system in terms of continuous media that meet at well-defined boundaries, by partitioning the system into a fine mesh of elementary volumes of size  $dV$ , each of which is homogeneous in the thermodynamic limit. Once the continuum scale of  $dV$  is identified, the dynamics is governed by conservation laws in the form of differential continuity equations for mass, particle number, momentum and energy, expressed in terms of fluxes and source densities defined throughout these media. These continuity equations are closed by assuming that each elementary volume is in local thermodynamic equilibrium (LTE), yielding linear constitutive relations between fluxes and gradients of certain thermodynamic and hydrodynamic continuum fields.[1] Within Onsager's theory of non-equilibrium thermodynamics, time-reversal symmetry implies that the transport coefficients in these relations are symmetric, a result known as the Onsager reciprocal relations.[2, 3] However, in non-equilibrium thermodynamics these coefficients are phenomenological quantities, dependent on molecular dynamic correlations and hence only inferable from experiments or from molecular dynamical simulations. This presents a limitation for describing the dynamics in colloidal suspensions, where molecular-level modeling is impractical.

To overcome this limitation, Derjaguin modelled the constituent particles of a medium as continuous objects on their own, thus obtaining continuum-mechanical expressions of transport coefficients based on

Onsager reciprocal symmetry.[4] This approach reduces the phenomenological character of coupling in the low Knudsen number regime, where the molecular dynamic effect on transport is captured by well-defined boundary conditions. However, since the underlying continuity equations are generally not time-reversible, such Onsager reciprocal approaches effectively postulate reciprocal symmetry at the continuum scale,[5] without clarifying the solvent’s role in momentum relaxation.[6] From a continuum-mechanical perspective, such a reciprocal symmetry is justified by the principle of kinematic reversibility, which is a prerequisite for applying the Lorentz reciprocal theorem (LRT). In contrast, continuum-mechanical reciprocal approaches often treat the underlying driving forces phenomenologically within a boundary layer approximation (BLA), based on an effective slip velocity[7] or interfacial tension gradient,[8] despite the fact that these may be related to thermodynamic equations of state. Indeed, an accurate prediction of phoretic mobilities relies on fully resolving the coupling between thermodynamic forces and hydrodynamic flows beyond the BLA, especially when the colloidal radius is comparable to its interfacial excess layer thickness.[9] Reducing the phenomenological character of colloidal transport thus remains a challenging area of active research, as evidenced by recent applications of the LRT, which often focus on force-free transport of a single colloid while assuming a no-slip hydrodynamic boundary condition at its surface.[10, 11, 12, 13]

## 2 Summary of main results

Here, we demonstrate that the aforementioned restrictions are not necessary when the LRT is applied to a representative volume element of the suspension, rather than the fluid region alone, based on the auxiliary flow problem of colloidal sedimentation. Although we focus our argumentation and derivation on purely translational motion, the resulting framework should also be applicable to rotational motion. Our approach provides a clear perspective on the underlying assumptions of kinematic reversibility, the solvent’s role in momentum relaxation, and the driving forces governing diffusion and advection in colloidal suspensions. In particular, we show that for a colloid of hydrodynamic radius  $R$  in a solution of viscosity  $\eta$ , the diffusiophoretic velocity  $\mathbf{v}_\Delta$  due to exclusion of an ideal solute from a region of radius  $R + \lambda$  around its hydrodynamic centre takes the form

$$\mathbf{v}_\Delta = -\frac{R^2}{9s\eta} \left[ 2x^3 + 2(1+x)^3 - 3x^2(s-2) - \frac{9}{2}s(1+x)^2 - 6(s-1)x + \frac{9}{2}s - 3 \right] k_B T \nabla n^b, \quad (1)$$

where  $x = \lambda/R$  and where  $2/3 \leq s \leq 1$  is the hydrodynamic slip parameter, whose value is determined by the hydrodynamic boundary condition at the colloidal surface. The osmotic pressure gradient is given by  $k_B T \nabla n^b$ , where  $T$  is the temperature and  $k_B$  is the Boltzmann constant, and is due to a gradient in solute number density  $n^b$  imposed in the bulk of the solution. In contrast to the classical result by Anderson,[7] this expression yields a zeroth-order contribution in the BLA ( $x \ll 1$ ) that drives the colloid towards higher bulk solute concentration, given by

$$\mathbf{v}_\Delta = \frac{R^2}{9s\eta} k_B T \nabla n^b. \quad (2)$$

As we will show, this contribution stems from a diffusive polarisation of solute around the colloid, due to the interfacial boundary condition of zero normal solute diffusion flux. More generally, we also demonstrate that Onsager reciprocal relations in colloidal diffusion do not need to be postulated: they emerge directly from the symmetry of the LRT, provided that hydrostatic and hydrodynamic stresses are carefully decoupled within a suspension at LTE.

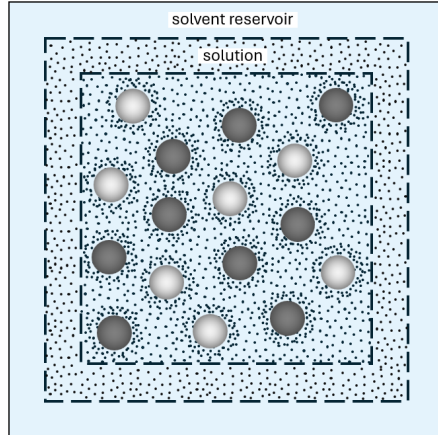


Figure 1: Schematic representation of a suspension. The dark and light gray spheres represent different species of microparticles, consisting of different solid microphases and suspended in a solution. The solution consists of small solutes (black dots) dispersed in a solvent reservoir. If the dark gray spheres are the colloids, then the fluid comprises the solution and the light gray spheres. The dashed lines represent thermodynamic reservoir boundaries.

### 3 Colloidal Suspensions: Preliminaries

#### 3.1 The system

The system under consideration is a volume-filling, incompressible colloidal suspension, which may include chemical or thermal sources, but must conserve mass internally. The local dynamics is described continuum-mechanically at a microscopic scale, relative to an inertial laboratory frame. On that scale, we refer to a collection of indistinguishable particles of a given chemical species as a component of the suspension, and define a microphase as a continuous medium composed of a combination of such components. As shown in Fig. 1, the suspension consists of different species of microparticles and small solutes dispersed in a solvent reservoir, such that within a mesoscopic representative volume element  $\mathcal{V}$  of volume  $V = L^3$  inside the suspension, we have  $N_c \ll N_k \ll N_l$ , where  $N_c$  is the number of microparticles of any microparticle species  $c$ ,  $N_k$  is the number of particles of any solute component  $k$ , and  $N_l$  is the number of particles of any solvent component  $l$ . In what follows, the indices  $c$ ,  $k$  and  $l$  are reserved for these entities, whereas the general indices  $i$  and  $j$  are used to refer to any set of components.

The solvent and the small solutes suspended in it constitute an isotropic viscous microphase (" $\eta$ ") known as the solution, occupying a partial region  $\nu_\eta$  within  $\mathcal{V}$ , whereas the microparticles (" $m$ ") occupy a partial region  $\nu_m = \mathcal{V} \setminus \nu_\eta$  of volume  $V_m$ . Each microparticle species consists of solid microphase, made of chemically bound components that do not support viscous shear or diffusion. The solution meets the surfaces of the microparticles at well-defined interfacial boundaries, where it remains isotropic assuming that molecular crowding and orientational correlations can be ignored. The colloids (" $c$ ") are a chosen species of microparticles whose motion we seek to determine, specified by a given index value  $c$  and occupying a partial region  $\nu_c$  of volume  $V_c$ , such that  $\nu_m = \bigcap_c \nu_c$  and  $V_m = \sum_c V_c$ . The fluid (" $\sim$ ") refers to the surrounding solution and all other microparticle species suspended in it, excluding the colloids and thus occupying a partial region  $\tilde{\nu} = \mathcal{V} \setminus \nu_c$ .

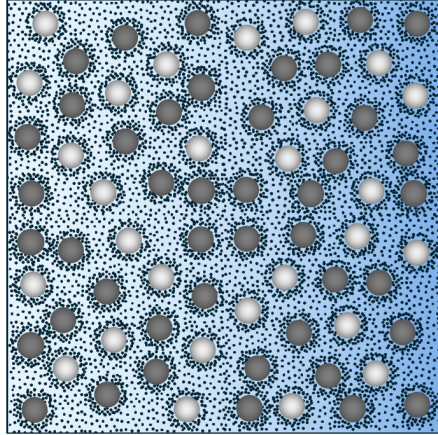


Figure 2: A representative volume element of a homogeneous suspension. The blue background gradient shows that the volume element is subjected to forces due to non-equilibrium boundary conditions.

The principle of kinematic reversibility is based on a low Knudsen number, low Reynolds number, and low Mach number, which are all tied to the solvent's role in momentum balance. The solvent is therefore modeled as a strongly coupled, highly viscous, molecular medium, forming a thermodynamic reservoir and rapidly responding to non-equilibrium forces to maintain a mechanical equilibrium under incompressible flow. Additionally, kinematic reversibility requires that two distinct flow fields defined within the same region must occur under the same dynamic viscosity and component number densities. This requirement, which is essential for the symmetry arguments involved in deriving the LRT, does not imply spatial uniformity of these quantities, but rather that they remain unchanged under different force fields. The condition of LTE must therefore hold not only at the continuum scale of  $dV$ , but also at the mesoscopic scale of a representative volume element  $\mathcal{V}$  of the suspension, which is therefore also treated as statistically homogeneous. In the dilute limit of such a suspension, when all microparticle species are present at low volume fractions, one then recovers the case of a single colloid suspended in a solution inside an unbounded representative volume element. This condition of representative local thermodynamic equilibrium (RLTE) justifies a decomposition into hydrostatic and hydrodynamic stress and allows for an equilibrium-statistical consideration of local component distributions. For a local continuum field  $\mathbf{q}$ , the corresponding equilibrium field is denoted by  $\mathbf{q}^{\text{eq}}$ . Furthermore, RLTE also ensures that boundary dynamics are slow compared to the relaxation of local continuum fields. As a result, local continuity equations are linear and solved under quasi-stationary boundary conditions on the internal and external boundaries of a representative volume element  $\mathcal{V}$ .

### 3.2 Homogenisation and continuity equations

Two different kinds of disturbances are of interest in colloidal transport. On one hand, force-free phoretic motion stems from continuum-mechanical disturbances induced by the colloids relative to the bulk fluid (" $b$ "), which corresponds to the hypothetical reference state of a representative volume element  $\mathcal{V}$  obtained by replacing the colloids inside  $\mathcal{V}$  by fluid. The disturbance of a field  $\mathbf{q}$  induced by the colloids relative to the bulk fluid is defined by

$$\delta\mathbf{q} = \mathbf{q} - \mathbf{q}^b, \quad (3)$$

where  $\mathbf{q}^b$  is the field of the bulk fluid, defined everywhere inside  $\mathcal{V}$ . Based on Eq. (3), we also have  $\delta\nabla \cdot \mathbf{q} = \nabla \cdot \delta\mathbf{q}$  and  $\delta(g\mathbf{q}) = \delta g\mathbf{q} + g^b\delta\mathbf{q}$ , where  $g$  is a scalar. On the other hand, colloidal diffusion is described as a disturbance relative to the average motion, or advection, of the suspension. However, unlike diffusion in molecular mixtures, which is described relative to the barycentric reference frame,[1] the natural reference frame for colloidal diffusion is the one of zero mean volume flux. The underlying reason for this choice is that linear mesoscopic continuity equations can be obtained by averaging over a representative volume element  $\mathcal{V}$  of a homogeneous suspension.[14, 15] Hence, the system is divided into a mesh of such volume elements, each of size  $V$ . For a given volume element  $\mathcal{V}$ , as depicted in Fig. 2, let  $\nu_\alpha$  denote the partial region of volume  $V_\alpha$  occupied by a given medium  $\alpha$ , which may or may not be continuous. If the medium is homogeneous over  $\mathcal{V}$ , then the ensemble average, or mean-field, of  $\mathbf{q}$  over that medium inside  $\mathcal{V}$  is equal to the volume average over its partial region  $\nu_\alpha$ , [15] given by

$$\langle \mathbf{q} \rangle_{\nu_\alpha} = \frac{1}{V_\alpha} \int_{\nu_\alpha} \mathbf{q} d^3\mathbf{r}, \quad (4)$$

where  $\langle \mathbf{q} \rangle_{\nu_\alpha}$  is interpreted as a uniform field defined everywhere inside  $\mathcal{V}$ . The disturbance of  $\mathbf{q}$  relative to  $\langle \mathbf{q} \rangle_{\nu_\alpha}$  is then defined as

$$\mathbf{q}'_{\nu_\alpha} = \mathbf{q} - \langle \mathbf{q} \rangle_{\nu_\alpha}, \quad (5)$$

such that  $\langle \mathbf{q}'_{\nu_\alpha} \rangle_{\nu_\alpha} = 0$ . If  $\mathbf{q}$  is the flux of a conserved quantity, then the volume-averaged divergence of  $\mathbf{q}$  over a homogeneous medium is equal to the divergence of its partial volume average:

$$\langle \nabla \cdot \mathbf{q} \rangle_{\nu_\alpha} = \bar{\nabla} \cdot \langle \mathbf{q} \rangle_{\nu_\alpha}, \quad (6)$$

where  $\bar{\nabla}$  denotes the mesoscopic gradient defined over adjacent volume elements. For convenience, when considering the volume average over the entire suspension within  $\mathcal{V}$ , we simply write

$$\langle \mathbf{q} \rangle_{\mathcal{V}} = \langle \mathbf{q} \rangle. \quad (7)$$

The suspension volume average  $\langle \mathbf{q} \rangle$  can further be expressed as a weighted sum of partial volume averages, such that

$$\langle \mathbf{q} \rangle = \gamma_\alpha \langle \mathbf{q} \rangle_{\nu_\alpha} + (1 - \gamma_\alpha) \langle \mathbf{q} \rangle_{\mathcal{V} \setminus \nu_\alpha}, \quad (8)$$

where  $\gamma_\alpha = V_\alpha/V$  is the volume fraction of medium  $\alpha$  inside  $\mathcal{V}$ .

In colloidal suspensions, local energy transport occurs primarily via heat conduction and is much faster than the transport of particles. Conservation of energy can therefore be described using the steady-state form of the heat equation:

$$\nabla \cdot \mathbf{j}_q = Q, \quad (9)$$

where  $Q$  is the heat source density and  $\mathbf{j}_q = -\kappa\nabla T$  is the conductive heat flux, which couples to the gradient in temperature  $T$  via the thermal conductivity  $\kappa$ . At mechanical equilibrium, the local momentum continuity equation is given by[16]

$$\mathbf{f} + \nabla \cdot \boldsymbol{\sigma} = 0, \quad (10)$$

where  $\mathbf{f}$  is the body force density and  $\boldsymbol{\sigma}$  is the stress tensor. This equation is solved under the constraint of incompressible flow, expressed by

$$\nabla \cdot \mathbf{u} = 0, \quad (11)$$

where  $\mathbf{u}$  is the flow velocity of an elementary volume  $dV$ . Due to the condition of RLTE, interfacial regions, which contain an excess of free energy due to interfacial potential interactions, can be considered at equilibrium, and the local dynamics inside a microphase decouples into a description of its effective component

reservoir only.[17, 18, 19] The reservoir of any microphase, denoted by a superscript "r", is defined in the limit where interfacial potential interactions are absent. Denoting the interfacial interaction potentials collectively by  $\{\phi_j\}$ , where  $j$  is an index over all components, the effective reservoir number density  $n_i^r$  of a component  $i$  is defined by  $n_i^r = n_i(\{\phi_j\} = 0)$ , where  $n_i$  is the local number density of component  $i$ . Hence, the corresponding particle number continuity equation takes the form

$$\frac{\partial n_i^r}{\partial t} + \nabla \cdot \mathbf{J}_i = \Gamma_i, \quad (12)$$

where  $\mathbf{J}_i$  is the particle flux of component  $i$ , and  $\Gamma_i$  is the corresponding chemical source density accounting for local production or annihilation of particles due to chemical reactions. Furthermore, the particle flux  $\mathbf{J}_i$  can be expressed as

$$\mathbf{J}_i = n_i^r \mathbf{u} + \mathbf{j}_i, \quad (13)$$

where  $\mathbf{j}_i$  is the local diffusion flux of component  $i$ . If the index  $i$  refers to a component of a solid microphase ( $i \in \nu_m$ ), where diffusion is prohibited, we simply have  $\mathbf{j}_i = 0$ . Using Eqs. (13) and (11), Eq. (12) can also be written as  $\partial n_i^r / \partial t + \mathbf{u} \cdot \nabla n_i^r + \nabla \cdot \mathbf{j}_i = \Gamma_i$ . The term  $\mathbf{u} \cdot \nabla n_i^r$  is of second order in the non-equilibrium forces and therefore negligible at RLTE. When the index  $i$  refers to a component of the solution ( $i \in \nu_\eta$ ), the local conservation of particle number within  $\mathcal{V}$  thus reduces to a local diffusive steady-state condition, of the form

$$\nabla \cdot \mathbf{j}_i = \Gamma_i. \quad (14)$$

The diffusion fluxes  $\mathbf{j}_i$  describe motion relative to the flow velocity  $\mathbf{u}$ . There is no need to specify whether these local fluxes and flows are described within a barycentric or volume-averaged reference frame, as long as the chosen frame is consistent with the above continuity equations.

For a continuum-statistical framework of colloidal motion, mesoscopic continuity equations are needed to describe advection and to determine the boundary conditions on representative volume elements for the local steady-states governed by Eqs. (9) and (14). In a homogeneous suspension, the volume averages of Eqs. (9) and (12) over  $\mathcal{V}$  yield the following mesoscopic continuity equations for momentum, energy and particle number:

$$\bar{\nabla} \cdot \langle \mathbf{j}_q \rangle = \langle Q \rangle, \quad (15)$$

$$\frac{\partial \langle n_i^r \rangle}{\partial t} + \bar{\nabla} \cdot \langle \mathbf{J}_i \rangle = \langle \Gamma_i \rangle. \quad (16)$$

$$\langle \mathbf{f} \rangle + \bar{\nabla} \cdot \langle \boldsymbol{\sigma} \rangle = 0, \quad (17)$$

where the advective velocity  $\langle \mathbf{u} \rangle$  is determined by Eq. (17). To describe colloidal diffusion, we therefore decompose the flow inside the suspension into an advective flow and a diffusive flow, such that  $\mathbf{u} = \langle \mathbf{u} \rangle + \mathbf{u}'$ . The diffusion flow velocity  $\mathbf{u}'$  represents the flow velocity inside the reference frame of zero mean volume flux, such that

$$\langle \mathbf{u}' \rangle = 0. \quad (18)$$

Averaging Eq. (11) over  $\mathcal{V}$ , and using Eq. (6), we get

$$\bar{\nabla} \cdot \langle \mathbf{u} \rangle = 0, \quad (19)$$

which also implies  $\nabla \cdot \mathbf{u}' = 0$ , so that both the advective flow and diffusion flow are incompressible. In terms of advection and diffusion flow, the particle flux of component  $i$  now takes the form

$$\mathbf{J}_i = n_i^r \langle \mathbf{u} \rangle + n_i^r \mathbf{u}' + \mathbf{j}_i, \quad (20)$$

so that the corresponding mean particle flux  $\langle \mathbf{J}_i \rangle$  becomes

$$\langle \mathbf{J}_i \rangle = \langle n_i^r \rangle \langle \mathbf{u} \rangle + \mathcal{J}_i, \quad (21)$$

where

$$\mathcal{J}_i = \langle n_i^r \mathbf{u}' \rangle + \langle \mathbf{j}_i \rangle \quad (22)$$

is the mean diffusion flux and  $\langle n_i^r \mathbf{u}' \rangle$  is the mean diffusion flow of component  $i$ . To introduce the colloids as a mesoscopic component of the suspension, we can consider any given microparticle species  $c$ , such that  $N_c$  identical colloids occupy a partial region  $\nu_c$  of a homogeneous volume element  $\mathcal{V}$ . Note that the fluid surrounding these colloids may comprise other species of microparticles. As shown in appendix A, the colloidal continuity equation can then be expressed as

$$\frac{\partial n_c}{\partial t} + \langle \mathbf{u} \rangle \cdot \bar{\nabla} n_c + \bar{\nabla} \cdot \mathcal{J}_c = \Gamma_c, \quad (23)$$

where  $n_c = N_c/V$  is the colloidal number density,  $\Gamma_c$  is the corresponding chemical source density and  $\mathcal{J}_c$  is the colloidal diffusion flux. In appendix A, we also show that the mean diffusion flow of a solute or solvent component  $i$  can be expressed in terms of the microparticle diffusion fluxes, such that Eq. (16) becomes

$$\frac{\partial \langle n_i^r \rangle}{\partial t} + \langle \mathbf{u} \rangle \cdot \bar{\nabla} \langle n_i^r \rangle - \bar{\nabla} \cdot \left( \bar{V}_m \langle n_i^r |^{\text{eq}} \rangle_{\nu_\eta} \sum_c \mathcal{J}_c \right) + \bar{\nabla} \cdot \langle \mathbf{j}_i \rangle = \langle \Gamma_i \rangle, \quad (24)$$

where  $i$  only runs over the components of the solution ( $i \in \nu_\eta$ ) and where  $\bar{V}_m = V_m / \sum_c N_c$  is the average volume of a microparticle.

Generally, determining the motion of every individual colloid is challenging when the fluid contains other microparticles, which turn the dynamics into a many-body interaction problem. However, many industrial applications are not concerned with the motion of each colloid, but rather with the average dynamics of an ensemble of colloids. Homogenisation thus enables a continuum-statistical description of colloidal motion based on mesoscopic volume averaging over a homogeneous suspension. Disturbances that do not contribute to the colloidal dynamics vanish upon averaging, whereas those that do manifest as deviations from the average suspension dynamics. Here, we use the LRT to develop such a continuum-statistical description of colloidal dynamics under kinematic reversibility, and evidence its connection to Onsager's theory of non-equilibrium thermodynamics.

## 4 Thermodynamic forces and hydrodynamic stress in colloidal suspensions

To bridge the gap between continuum-mechanical and non-equilibrium thermodynamic reciprocal relations in colloidal motion, we must distinguish the forces that drive motion from those that respond to motion. Based on the condition of RLTE, we therefore decompose the stress tensor  $\boldsymbol{\sigma}$  into a hydrostatic stress  $\boldsymbol{\sigma}_s$ , and a hydrodynamic stress  $\boldsymbol{\sigma}_d$  that vanishes in a static suspension:[16]

$$\boldsymbol{\sigma} = \boldsymbol{\sigma}_s + \boldsymbol{\sigma}_d. \quad (25)$$

To obtain constitutive forms of the hydrostatic and hydrodynamic stress, we write the stress tensor  $\boldsymbol{\sigma}$  as

$$\boldsymbol{\sigma} = -P\mathbf{I} + \boldsymbol{\Sigma}, \quad (26)$$

where  $P = \text{Tr } \boldsymbol{\sigma} / 3$  is the pressure,  $\mathbf{I}$  is the identity tensor, and  $\boldsymbol{\Sigma}$  is the shear stress tensor. In suspensions,  $\boldsymbol{\Sigma}$  consists of a purely viscous stress  $\boldsymbol{\Sigma}_\eta$  inside the solution, and of a solid constraint stress  $\boldsymbol{\Sigma}_m$  inside the microparticles. We can therefore write the shear stress tensor as a sum of two separate stress fields, such that  $\boldsymbol{\Sigma} = \boldsymbol{\Sigma}_\eta + \boldsymbol{\Sigma}_m$ . The linear constitutive relation for the viscous stress tensor under incompressible flow is given by  $\boldsymbol{\Sigma}_\eta = \eta \mathbf{e}$ , where  $\eta$  is the dynamic viscosity of the solution, and  $\mathbf{e}$  is the strain rate tensor, defined by  $\mathbf{e} = (\nabla \mathbf{u} + \nabla^\dagger \mathbf{u}) / 2$ . Since the microparticles are only in direct contact with the solution and hence under isotropic hydrostatic stress, we obtain the constitutive forms

$$\boldsymbol{\sigma}_s = -P_s \mathbf{I}, \quad (27)$$

$$\boldsymbol{\sigma}_d = -P_d \mathbf{I} + \boldsymbol{\Sigma}_m + \boldsymbol{\Sigma}_\eta, \quad (28)$$

where  $P_s$  and  $P_d$  denote the hydrostatic and hydrodynamic pressure, respectively, such that  $P = P_s + P_d$ . Inside the solution, the hydrodynamic pressure  $P_d$  couples to the solvent reservoir and thereby acts as a Lagrange multiplier to enforce incompressible flow. To examine the hydrostatic response of the solvent reservoir, we write  $P_s$  as the sum of a hydrostatic solvent reservoir pressure  $p$  and an osmotic pressure  $\Pi$ : [17]

$$P_s = \Pi + p, \quad (29)$$

Inside the solution, the osmotic pressure  $\Pi$  stems from the presence of solutes and from local hydrostatic stresses induced at the interfacial boundaries, whereas in the microparticles, it coincides with the hydrostatic pressure  $P_s$ . Due to strong intermolecular coupling, the solvent components always remain in an internal hydrostatic equilibrium. As a result, the pressure of the solvent reservoir remains uniform unless it must respond to external forces on its components or to collisional interactions with other components. Crucially, the very existence of osmotic fluid flow in suspensions implies that the solvent reservoir favors a hydrodynamic response over a hydrostatic response. The solvent reservoir can therefore only enforce a hydrostatic equilibrium normal to a static boundary if momentum relaxation via viscous flow is prohibited ( $\nabla \cdot \boldsymbol{\sigma}_d = 0$ ). As a result, the hydrostatic solvent reservoir pressure  $\delta p$  induced by the colloids relative to the bulk fluid cannot drive colloidal motion, implying that

$$\oint_{\partial \nu_c} \delta p \mathbf{n} dS = 0, \quad (30)$$

where  $\mathbf{n}$  is the unit normal vector pointing out of the solid interfacial boundaries  $\partial \nu_c$  of the colloids.

In a suspension at RLTE, a local balance is maintained between the body forces and pressure forces arising from interfacial potential interactions. [20] The corresponding interfacial hydrostatic equilibrium is described by [6]

$$\sum_i \left( n_i^{\text{eq}} \nabla \phi_i + \frac{\partial P_s}{\partial \phi_i} \nabla \phi_i \right) = 0, \quad (31)$$

where  $n_i^{\text{eq}}$  is the equilibrium number density of component  $i$ . If Eq. (31) is subtracted from Eq. (10), then the body force  $\mathbf{F}_i$  on component  $i$  can be understood as stemming only from external fields or non-equilibrium boundary conditions. Consequently, the hydrostatic pressure gradient is then evaluated at constant interfacial interaction potentials. For a first-order evaluation, we can use the Gibbs-Duhem equation to write

$$\nabla_1 P_s = \left. \frac{\partial P_s}{\partial \mathbf{r}} \right|_{\{\phi_j\}}^{\text{eq}} = h^{\text{eq}} \frac{\nabla T}{T^{\text{eq}}} + \sum_i n_i^{\text{eq}} \nabla_T \mu_i, \quad (32)$$

where the subscript "1" indicates evaluation to first order in the thermodynamic forces.  $\nabla_T \mu_i$  is the gradient at constant temperature of the chemical potential  $\mu_i$  of component  $i$ . The modified equilibrium enthalpy

density  $h^{\text{eq}}$  is given by  $h^{\text{eq}} = \mathcal{H}^{\text{eq}} - \sum_i n_i^{\text{eq}} \check{H}_i$ , where  $\mathcal{H}$  is the net equilibrium enthalpy density and  $\check{H}_i$  is the partial enthalpy per particle of component  $i$ . [21] With Eqs. (29) and (32), the osmotic pressure gradient  $\nabla_1 \delta \Pi$  induced by the colloids can now be expressed as

$$\nabla_1 \delta \Pi = \delta h^{\text{eq}} \frac{\nabla T}{T^{\text{eq}}} + \sum_i \delta n_i^{\text{eq}} \nabla_T \mu_i + \left. \frac{\partial \Pi^b}{\partial T^b} \right|_{\text{eq}} \nabla \delta T + \sum_{i \neq l} n_i^{b|\text{eq}} \nabla_T \delta \mu_i. \quad (33)$$

Here,  $\delta h^{\text{eq}}$  and  $\delta n_i^{\text{eq}}$ , which respectively couple to the local thermodynamic forces  $\nabla T$  and  $\nabla_T \mu_i$ , correspond to the interfacial excess densities of enthalpy and component number arising from interfacial potential interactions between the fluid and the colloids. Eq. (33) shows that an osmotic pressure gradient can be induced not only due to these interfacial excess densities, but also due to disturbances of the thermodynamic forces  $\nabla T$  and  $\nabla_T \mu_i$  relative to the bulk fluid. Such disturbances arise when the internal transport properties of the colloids differ from those of the fluid. Crucially, the notation  $i \neq l$  in Eq. (33) indicates that such disturbances in the solvent do not contribute to the induced osmotic pressure gradient, based on the internal hydrostatic equilibrium of its components discussed earlier. The non-equilibrium body force density can be written as

$$\mathbf{f}_1 = \sum_i n_i^{\text{eq}} \mathbf{F}_i. \quad (34)$$

The non-equilibrium body force  $\mathbf{F}_i$  consists of an electric force and a gravitational force, such that  $\mathbf{F}_i = ez_i \mathbf{E} + m_i \mathbf{g}$ , where  $e$  is the elementary charge,  $z_i$  and  $m_i$  are the charge number and mass of a particle of component  $i$ , and  $\mathbf{E}$  and  $\mathbf{g}$  are the corresponding electric and gravitational field vectors. The gravitational field vector  $\mathbf{g}$  is uniform throughout the suspension. As mesoscopic charge separation is prohibited at RLTE, [20] the representative volume element  $\mathcal{V}$  must be overall electroneutral. Hence, the non-equilibrium electric field  $\mathbf{E}$  is decoupled from any interfacial excess charge densities and governed by the source-free form of Gauss' law to first order in the non-equilibrium forces:

$$\epsilon \nabla \cdot \mathbf{E} = 0. \quad (35)$$

For convenience, we introduce the thermodynamic force density via

$$\mathcal{F} = \mathbf{f}_1 - \nabla_1 P_s. \quad (36)$$

With Eqs. (25) and (36), the momentum continuity equation given by Eq. (10) becomes

$$\mathcal{F} + \nabla \cdot \boldsymbol{\sigma}_d = 0. \quad (37)$$

Introducing the mass density  $\rho = \sum_i m_i n_i^{\text{eq}}$  and electric charge density  $\omega = \sum_i ez_i n_i^{\text{eq}}$ , and using Eq. (29) in Eq. (36), we obtain the osmo-mechanical form of  $\mathcal{F}$ :

$$\mathcal{F} = \rho \mathbf{g} + \omega \mathbf{E} - \nabla_1 \Pi - \nabla_1 p, \quad (38)$$

whereas substitution of Eqs. (34) and (32) into Eq. (36) yields the non-equilibrium thermodynamic form of  $\mathcal{F}$ :

$$\mathcal{F} = -h^{\text{eq}} \frac{\nabla T}{T^{\text{eq}}} + \sum_i n_i^{\text{eq}} (\mathbf{F}_i - \nabla_T \mu_i). \quad (39)$$

The two forms given by Eqs. (38) and (39) provide a quantitative link between continuum-mechanical and thermodynamic forces. In the absence of interfacial potential interactions, the densities  $n_i^{\text{eq}}$  and  $h^{\text{eq}}$  reduce to equilibrium reservoir densities  $n_i^{r|\text{eq}}$  and  $h^{r|\text{eq}}$ , respectively, which are uniform inside a given microphase. The

chemical potentials  $\mu_i$  are local state functions of temperature  $T$  and reservoir number densities  $\{n_j^r\}$ , but are independent of interfacial interaction potentials. The vectorial thermodynamic forces  $-\nabla T/T_{\text{eq}}$  and  $\mathbf{F}_i - \nabla_T \mu_i$  are determined by Eqs. (14), (9) and (35) under quasi-stationary boundary conditions and are uniform across  $\mathcal{V}$  in the absence of any interfacial boundary conditions within  $\mathcal{V}$ . The Curie symmetry principle further implies that the diffusion fluxes within an isotropic solution only couple to vectorial thermodynamic forces.[1] Since the solvent reservoir is fixed by the condition of incompressibility, these diffusion fluxes must only be considered for the solute components:

$$\mathbf{j}_k = -L_{kq} \frac{\nabla T}{T_{\text{eq}}} + \sum_{j \in \nu_\eta} L_{kj} (\mathbf{F}_k - \nabla_T \mu_k). \quad (40)$$

Like the equilibrium densities  $n_i^{\text{eq}}$  and  $h^{\text{eq}}$ , the Onsager transport coefficients  $L_{kj}$  and  $L_{kq}$  are sensitive to interfacial potential interactions, but are evaluated at equilibrium. As a result, the thermodynamic force density  $\mathcal{F}$  and diffusion fluxes  $\mathbf{j}_k$  are indeed linear in the thermodynamic forces. For the diagonal Onsager coefficients, we have

$$L_{kk} = \frac{n_k^{\text{eq}}}{\xi_k}, \quad (41)$$

where  $\xi_k$  is the friction coefficient of a particle of solute component  $k$ . Crucially, the cross-coupling coefficients in Eq. (40) satisfy the Onsager reciprocal relations

$$L_{kq} = L_{qk}, \quad (42)$$

$$L_{kj} = L_{jk}, \quad (43)$$

implying that they also describe the heat flux and diffusion flux of component  $j$  caused by a body force on solute component  $k$ , respectively. In contrast to Eq. (38), Eq. (39) directly maps  $\mathcal{F}$  onto the constitutive form of the diffusion fluxes given by Eq. (40), which is useful to reduce the number of independent thermodynamic forces when solute components have reached global steady-states. However, only Eq. (38) isolates the hydrostatic pressure gradient  $\nabla_1 p$  of the solvent reservoir, which is necessary to properly account for the solvent reservoir response in colloidal motion.

As shown in appendix A, the decomposition of hydrostatic pressure given by Eq. (29) can be used to write the mesoscopic momentum balance equation as

$$\langle \rho \rangle \mathbf{g} - \langle \nabla_1 \Pi \rangle - (1 - \gamma_m) \bar{\nabla} \bar{p} + \bar{\nabla} \cdot \langle \boldsymbol{\sigma}_d \rangle = 0, \quad (44)$$

where  $\gamma_m = V_m/V$  is the microparticle volume fraction and  $\bar{p} = \langle p \rangle_{\nu_\eta}$  is the solution-averaged hydrostatic pressure of the solvent reservoir. Eq. (44) coincides with a result reported elsewhere[15] and reduces to a description of advection inside a bulk solution in the dilute limit. In particular, hydrodynamic stress disturbances decay with distance from a microparticle and, in a homogeneous suspension, are statistically invariant under translation. The divergence of the hydrodynamic suspension stress  $\langle \boldsymbol{\sigma}_d \rangle$  therefore reduces to

$$\bar{\nabla} \cdot \langle \boldsymbol{\sigma}_d \rangle = \bar{\nabla} \cdot (-\bar{P}_d \mathbf{I} + \bar{\eta} \langle \mathbf{e} \rangle), \quad (45)$$

where  $\bar{P}_d$  is the hydrodynamic suspension pressure,  $\bar{\eta}$  is the dynamic viscosity of the suspension, and  $\langle \mathbf{e} \rangle$  is the strain rate tensor of the advective velocity  $\langle \mathbf{u} \rangle$ . The hydrodynamic suspension pressure  $\bar{P}_d$  couples to the solvent reservoir to enforce incompressible advection according to Eq. (19). Eq. (44) can be solved for the advective velocity  $\langle \mathbf{u} \rangle$  under known boundary conditions and driving forces of advection, which consist of

the volume-averaged gravitational force density and osmotic pressure gradient. If advective flow is permitted and  $\bar{\nabla}\bar{p} = 0$ , then Eq. (44) becomes

$$\langle \rho \rangle \mathbf{g} - \langle \nabla_1 \Pi \rangle - \bar{\nabla} \cdot \langle \boldsymbol{\sigma}_d \rangle = 0, \quad (46)$$

whereas in a suspension at hydrostatic equilibrium, it reduces to

$$\langle \rho \rangle \mathbf{g} - \langle \nabla_1 \Pi \rangle - (1 - \gamma_m) \bar{\nabla} \bar{p} = 0, \quad (47)$$

which fixes the mean hydrostatic solvent reservoir pressure gradient under purely diffusive motion. In this context, it is instructive to consider two suspensions at hydrostatic equilibrium, contained in two separate vessels open at the top and connected by a narrow horizontal channel of length  $L$  (aligned along  $x$ ) that permits only solvent to pass. If the hydrostatic pressures of the suspensions are equal at the height  $z_0$  of the channel, then a solvent pressure gradient is established along the channel, such that  $\partial \bar{p} / \partial x = -\Delta \langle \bar{\Pi} \rangle / L$ , where  $\Delta \langle \bar{\Pi} \rangle = \langle \bar{\Pi} \rangle_{L, z_0} - \langle \bar{\Pi} \rangle_{0, z_0}$  is the osmotic pressure difference between the suspensions. Projection of Eq. (44) onto  $x$  then yields  $-\partial \bar{p} / \partial x + \bar{\nabla} \cdot \langle \boldsymbol{\sigma}_d \rangle = 0$ , or alternatively

$$\Delta \langle \bar{\Pi} \rangle + L \bar{\nabla} \cdot \langle \boldsymbol{\sigma}_d \rangle = 0. \quad (48)$$

This momentum balance equation describes the effect of classical osmosis through a semi-permeable channel or membrane, driving solvent flow into the vessel at higher osmotic pressure.

To complete our framework, we require closed continuum-statistical forms of the diffusion fluxes that govern the component distributions. To complete our framework, we require closed continuum-statistical forms of the diffusion fluxes that govern the component distributions. The aim of this work is to show that this can be achieved with the LRT using the auxiliary flow problem of colloidal sedimentation.

## 5 Reciprocal formulation of colloidal diffusion

Our aim is to derive a closed form of the volume-averaged velocity  $\mathbf{v}_c$  of an ensemble of  $N_c$  colloids inside a representative volume element  $\mathcal{V}$  at RLTE, defined by

$$\mathbf{v}_c = \langle \mathbf{u} \rangle_{\nu_c}. \quad (49)$$

To this end, we consider the auxiliary flow problem ("\*") of colloidal sedimentation, where a uniform body force  $\mathbf{F}^*$  is applied to every colloid, corresponding to a momentum continuity equation

$$\mathbf{f}^* + \nabla \cdot \boldsymbol{\sigma}_d^* = 0, \quad (50)$$

where  $\mathbf{f}^*$  takes the value  $N_c \mathbf{F}^* / V_c$  inside the colloids and zero elsewhere. The flow induced by sedimentation is a flow of zero mean volume flux, such that

$$\langle \mathbf{u}^* \rangle = 0. \quad (51)$$

Each colloid sediments at a given velocity that may vary across the ensemble. The force  $\mathbf{F}^*$  is therefore chosen so that the mean sedimentation velocity equals the colloidal velocity  $\mathbf{v}_c$ :

$$\langle \mathbf{u}^* \rangle_{\nu_c} = \mathbf{v}_c. \quad (52)$$

In a homogeneous suspension under kinematic reversibility, the flow velocity and hydrodynamic stress are described by tensorial relations that are linear in  $\mathbf{v}_c$ . [16, 14] We can therefore write

$$\mathbf{u}^* = \mathbf{U}_c^* \cdot \mathbf{v}_c, \quad (53)$$

$$\boldsymbol{\sigma}_d^* = \mathcal{P}_c^* \cdot \mathbf{v}_c, \quad (54)$$

where  $\mathbf{U}_c^*$  and  $\mathcal{P}_c^*$  are the symmetric Stokes flow tensor and Stokes stress tensor, respectively. The Stokes flow tensor  $\mathbf{U}_c^*$  satisfies

$$\nabla \cdot \mathbf{U}_c^* = 0, \quad (55)$$

$$\langle \mathbf{U}_c^* \rangle = 0, \quad (56)$$

$$\langle \mathbf{U}_c^* \rangle_{\nu_c} = \mathbf{I}. \quad (57)$$

Furthermore, we have  $\mathbf{F}^* = \boldsymbol{\xi}_c \cdot \mathbf{v}_c$ , where the Stokes friction tensor  $\boldsymbol{\xi}_c$  of the colloids is related to the hydrodynamic traction tensor  $\boldsymbol{\Lambda}_c^* = \mathcal{P}_c^* \cdot \mathbf{n}$  via

$$N_c \boldsymbol{\xi}_c = - \oint_{\partial \nu_c} \boldsymbol{\Lambda}_c^* dS = - \oint_{\partial \nu} \boldsymbol{\Lambda}_c^* dS, \quad (58)$$

where the last equality follows from the momentum continuity equation  $\nabla \cdot \boldsymbol{\sigma}_d^* = 0$  inside the fluid.

To derive the LRT for a representative volume element of a colloidal suspension, we first follow the standard procedure of contracting the forces from the momentum continuity equation of each problem with the velocity field of the other problem. [16, 22] However, instead of using the Cauchy form of the momentum continuity equation, as given by Eq. (10), we use its form in terms of the thermodynamic force density and hydrodynamic stress, given by Eq. (37). Since both contractions are zero, equating them gives

$$\mathbf{u} \cdot (\mathbf{f}^* + \nabla \cdot \boldsymbol{\sigma}_d^*) = \mathbf{u}^* \cdot (\mathcal{F} + \nabla \cdot \boldsymbol{\sigma}_d). \quad (59)$$

Collecting the terms related to hydrodynamic stresses  $\boldsymbol{\sigma}_d$  and  $\boldsymbol{\sigma}_d^*$  on the right-hand side, we obtain

$$\mathbf{u}^* \cdot \mathcal{F} - \mathbf{u} \cdot \mathbf{f}^* = \mathbf{u} \cdot (\nabla \cdot \boldsymbol{\sigma}_d^*) - \mathbf{u}^* \cdot (\nabla \cdot \boldsymbol{\sigma}_d). \quad (60)$$

Each term on the right-hand side can further be rewritten using the identity  $\mathbf{u} \cdot (\nabla \cdot \boldsymbol{\sigma}) = \nabla \cdot (\mathbf{u} \cdot \boldsymbol{\sigma}) - \boldsymbol{\sigma} : \nabla \mathbf{u}$ , yielding  $\mathbf{u}^* \cdot \mathcal{F} - \mathbf{u} \cdot \mathbf{f}^* = \nabla \cdot (\mathbf{u} \cdot \boldsymbol{\sigma}_d^* - \mathbf{u}^* \cdot \boldsymbol{\sigma}_d) + \boldsymbol{\sigma}_d : \nabla \mathbf{u}^* - \boldsymbol{\sigma}_d^* : \nabla \mathbf{u}$ . The LRT relies on the symmetry of the last two terms in this relation. Using the incompressibility condition given by Eq. (11) and the constitutive form of the hydrodynamic stress given by Eq. (28) in both flow problems, we have  $\boldsymbol{\sigma}_d : \nabla \mathbf{u}^* = \boldsymbol{\Sigma}_m : \nabla \mathbf{u}^* + 2\eta \mathbf{e} : \mathbf{e}^*$ . As the dynamic viscosity  $\eta$  is the same in both flow problems under kinematic reversibility, the last term on the right-hand side is symmetric in the interchange of  $\mathbf{e}$  and  $\mathbf{e}^*$ . We can therefore write  $\boldsymbol{\sigma}_d : \nabla \mathbf{u}^* - \boldsymbol{\sigma}_d^* : \nabla \mathbf{u} = \boldsymbol{\Sigma}_m : \nabla \mathbf{u}^* - \boldsymbol{\Sigma}_m^* : \nabla \mathbf{u}$ . However, the terms on the right-hand side only refer to regions of  $\mathcal{V}$  occupied by the microparticles, inside which flow velocity gradients are forbidden. Hence,

$$\boldsymbol{\sigma}_d : \nabla \mathbf{u}^* - \boldsymbol{\sigma}_d^* : \nabla \mathbf{u} = 0, \quad (61)$$

and Eq. (60) reduces to

$$\mathbf{u}^* \cdot \mathcal{F} - \mathbf{u} \cdot \mathbf{f}^* = \nabla \cdot (\mathbf{u} \cdot \boldsymbol{\sigma}_d^* - \mathbf{u}^* \cdot \boldsymbol{\sigma}_d). \quad (62)$$

Eq. (62) is independent of the flow velocity gradient  $\nabla \mathbf{u}$  and can therefore be seen as a continuum-mechanical manifestation of the Curie symmetry principle.

In contrast to other works,[16, 10, 12, 13] where Eq. (62) is integrated over the partial volume of the fluid only, we integrate it over the entire representative volume element  $\mathcal{V}$ , giving

$$\underbrace{\int_{\mathcal{V}} \mathbf{u}^* \cdot \mathcal{F} d^3\mathbf{r}}_{I_1} - \underbrace{\int_{\mathcal{V}} \mathbf{u} \cdot \mathbf{f}^* d^3\mathbf{r}}_{I_2} = \underbrace{\int_{\mathcal{V}} \nabla \cdot (\mathbf{u} \cdot \boldsymbol{\sigma}_d^* - \mathbf{u}^* \cdot \boldsymbol{\sigma}_d) d^3\mathbf{r}}_{I_3}. \quad (63)$$

Based on the relations for the auxiliary flow problem, integrals  $I_1$  and  $I_2$  can be re-expressed as

$$I_1 = \mathbf{v}_c \cdot \int_{\mathcal{V}} \mathbf{U}_c^* \cdot \mathcal{F} d^3\mathbf{r}, \quad (64)$$

$$I_2 = N_c \mathbf{v}_c \cdot \boldsymbol{\xi}_c \cdot \mathbf{v}_c. \quad (65)$$

Moreover, applying Gauss' theorem to integral  $I_3$  yields

$$I_3 = \oint_{\partial\mathcal{V}} (\mathbf{u} \cdot \boldsymbol{\sigma}_d^* - \mathbf{u}^* \cdot \boldsymbol{\sigma}_d) \cdot \mathbf{n} dS - \oint_{\partial\nu_m} (\mathbf{u}^{\parallel} \cdot \boldsymbol{\sigma}_d^* - \mathbf{u}^{\parallel*} \cdot \boldsymbol{\sigma}_d) \cdot \mathbf{n} dS, \quad (66)$$

where  $\mathbf{u}^{\parallel}$  and  $\mathbf{u}^{\parallel*}$  are tangential slip velocities at the surfaces  $\partial\nu_m$  of the microparticles in each flow problem. As thermal transpiration is negligible at low Knudsen number,[23] these slip velocities satisfy the Navier slip boundary condition:[24]

$$\mathbf{u}^{\parallel} = \mathbf{u}_a + \frac{l_{\text{slip}}}{\eta} (\mathbf{I} - \mathbf{n}\mathbf{n}) \cdot (\mathbf{n} \cdot \boldsymbol{\sigma}_d), \quad (67)$$

$$\mathbf{u}^{\parallel*} = \frac{l_{\text{slip}}}{\eta} (\mathbf{I} - \mathbf{n}\mathbf{n}) \cdot (\mathbf{n} \cdot \boldsymbol{\sigma}_d^*). \quad (68)$$

In the actual flow problem, the active slip velocity profile  $\mathbf{u}_a$  is defined on all microparticle surfaces. In our treatment, this active slip velocity represents a boundary layer treatment of force-free self-propulsion mechanisms stemming only from non-hydrostatic forces that are not captured by the thermodynamic force density  $\mathcal{F}$ , like those giving rise to microswimming.[25, 26] As for dynamic viscosity, the principle of kinematic reversibility justifies the use of the same hydrodynamic slip length  $l_{\text{slip}}$  in both flow problems. Let us consider the integral of the term  $\mathbf{u}^{\parallel} \cdot \boldsymbol{\sigma}_d^* \cdot \mathbf{n}$  over the interfaces in Eq. (66). Substituting Eq. (67), we can write  $((\mathbf{I} - \mathbf{n}\mathbf{n}) \cdot (\mathbf{n} \cdot \boldsymbol{\sigma}_d) \cdot \boldsymbol{\sigma}_d^*) \cdot \mathbf{n} = (\mathbf{n} \cdot \boldsymbol{\sigma}_d) \cdot (\mathbf{n} \cdot \boldsymbol{\sigma}_d^*) - (\mathbf{n} \cdot \boldsymbol{\sigma}_d \cdot \mathbf{n}) \cdot (\mathbf{n} \cdot \boldsymbol{\sigma}_d^* \cdot \mathbf{n})$ , which is symmetric in the interchange of  $\boldsymbol{\sigma}_d$  and  $\boldsymbol{\sigma}_d^*$ . Hence, we obtain

$$\oint_{\partial\nu_m} (\mathbf{u}^{\parallel} \cdot \boldsymbol{\sigma}_d^* - \mathbf{u}^{\parallel*} \cdot \boldsymbol{\sigma}_d) \cdot \mathbf{n} dS = \mathbf{v}_c \cdot \oint_{\partial\nu_m} \boldsymbol{\Lambda}_c^* \cdot \mathbf{u}_a dS. \quad (69)$$

To describe colloidal diffusion, we introduce the decompositions  $\mathbf{u} = \mathbf{u}' + \langle \mathbf{u} \rangle$  and  $\boldsymbol{\sigma}_d = \boldsymbol{\sigma}_d' + \langle \boldsymbol{\sigma}_d \rangle$  into the surface integral over  $\partial\mathcal{V}$ , giving

$$\oint_{\partial\mathcal{V}} (\mathbf{u} \cdot \boldsymbol{\sigma}_d^* - \mathbf{u}^* \cdot \boldsymbol{\sigma}_d) \cdot \mathbf{n} dS = -\mathbf{v}_c \cdot N_c \boldsymbol{\xi}_c \cdot \langle \mathbf{u} \rangle + \oint_{\partial\mathcal{V}} (\mathbf{u}' \cdot \boldsymbol{\sigma}_d^* - \mathbf{u}^* \cdot \boldsymbol{\sigma}_d') \cdot \mathbf{n} dS, \quad (70)$$

where  $\langle \mathbf{u} \rangle$  is the advective velocity. For a single colloid, the flow velocities  $\mathbf{u}'$  and  $\mathbf{u}^*$  and hydrodynamic stress tensors  $\boldsymbol{\sigma}_d'$  and  $\boldsymbol{\sigma}_d^*$  are known to decay as  $1/r$  and  $1/r^2$  inside the solution, respectively,[16, 27] implying that the surface integrals over  $\partial\mathcal{V}$  in Eq. (70) vanish as the boundaries of  $\mathcal{V}$  tend to infinity. For a homogeneous

suspension, the vanishing of these surface integrals is instead justified by the statistical invariance of these quantities under translation. We therefore have

$$\oint_{\partial\mathcal{V}} (\mathbf{u}' \cdot \boldsymbol{\sigma}'_d - \mathbf{u}^* \cdot \boldsymbol{\sigma}'_d) \cdot \mathbf{n} \, dS = 0. \quad (71)$$

Crucially, Eqs. (69) and (71) rely on these specific properties of hydrodynamic stress, which highlights the necessity of decoupling it from hydrostatic stress. Integral  $I_3$  thus reduces to

$$I_3 = -\mathbf{v}_c \cdot N_c \boldsymbol{\xi}_c \cdot \langle \mathbf{u} \rangle - \mathbf{v}_c \cdot \oint_{\partial\nu_m} \boldsymbol{\Lambda}_c^* \cdot \mathbf{u}_a \, dS. \quad (72)$$

Using Eqs. (64), (65) and (72) in Eq. (63), the colloidal velocity relative to advection, or colloidal diffusion velocity, can be identified as

$$\mathbf{v}_c - \langle \mathbf{u} \rangle = \frac{1}{N_c \boldsymbol{\xi}_c} \cdot \left( \int_{\mathcal{V}} \mathbf{U}_c^* \cdot \mathcal{F} \, d^3\mathbf{r} + \oint_{\partial\nu_m} \boldsymbol{\Lambda}_c^* \cdot \mathbf{u}_a \, dS \right). \quad (73)$$

The colloidal diffusion flux  $\mathcal{J}_c$  is then related to the colloidal diffusion velocity via

$$\mathcal{J}_c = \frac{N_c}{V} (\mathbf{v}_c - \langle \mathbf{u} \rangle). \quad (74)$$

Notably, the colloidal diffusion velocity  $\mathbf{v}_c - \langle \mathbf{u} \rangle$  only refers to the hydrodynamic tensors  $\mathbf{U}_c^*$  and  $\boldsymbol{\Lambda}_c^*$  of the auxiliary Stokes problem of colloidal sedimentation, which are well established and feasible to determine numerically. In the fluid region, these tensors account for the hydrodynamic drag on the colloid due to forces on the fluid components. This hydrodynamic drag vanishes in the limit where the colloid's hydrodynamic radius tends to zero, which is also known as the Hückel limit. The first term in Eq. (73) describes diffusion due to vectorial thermodynamic forces, including sedimentation and force-free phoretic transport due to externally applied or self-generated gradients. The second term represents diffusion due to microswimming, accounting for the force on the colloids induced by non-hydrostatic self-propulsion of any microparticle species. For self-propulsion, which includes microswimming and self-phoretic transport, it is also worth noting that the resulting coupling between stresses and thermal fluctuations can induce spatial and orientational correlations that eventually lead to a breakdown of homogeneity and isotropy inside the suspension.

To evidence the connection to Onsager's reciprocal theory, we now substitute Eq. (39) into Eq. (73), yielding

$$\mathcal{J}_c = -\frac{1}{\boldsymbol{\xi}_c} \cdot \left\langle h^{\text{eq}} \mathbf{U}_c^* \cdot \frac{\nabla T}{T^{\text{eq}}} \right\rangle + \frac{1}{\boldsymbol{\xi}_c} \cdot \sum_i \langle n_i^{\text{eq}} \mathbf{U}_c^* \cdot (\mathbf{F}_i - \nabla_T \mu_i) \rangle + \frac{1}{\boldsymbol{\xi}_c} \cdot \oint_{\partial\nu_m} \boldsymbol{\Lambda}_c^* \cdot \mathbf{u}_a \, dS. \quad (75)$$

Indeed, the quantities  $h^{\text{eq}} \mathbf{U}_c^*$  and  $n_i^{\text{eq}} \mathbf{U}_c^*$  can be identified as the local flows of heat and component particles induced by colloidal sedimentation, respectively. If the thermodynamic forces are assumed uniform over  $\mathcal{V}$ , we obtain

$$\mathcal{J}_c = -\mathbf{L}_{cq} \cdot \frac{\nabla T}{T^{\text{eq}}} + \sum_i \mathbf{L}_{ci} \cdot (\mathbf{F}_i - \nabla_T \mu_i) + \frac{1}{\boldsymbol{\xi}_c} \cdot \oint_{\partial\nu_m} \boldsymbol{\Lambda}_c^* \cdot \mathbf{u}_a \, dS, \quad (76)$$

with  $\mathbf{L}_{cq} = \boldsymbol{\xi}_c^{-1} \cdot \langle h^{\text{eq}} \mathbf{U}_c^* \rangle$  and  $\mathbf{L}_{ci} = \boldsymbol{\xi}_c^{-1} \cdot \langle n_i^{\text{eq}} \mathbf{U}_c^* \rangle$ . Since transport tensors must reduce to scalars in a homogeneous, isotropic suspension, such that  $\mathbf{L}_{cq} = L_{cq} \mathbf{I}$ ,  $\mathbf{L}_{ci} = L_{ci} \mathbf{I}$  and  $\boldsymbol{\xi}_c = \xi_c \mathbf{I}$ , we finally recover the

standard scalar form of the Onsager reciprocal relations for colloidal diffusion:

$$L_{cq} = L_{qc} = \frac{1}{\xi_c} \langle h^{\text{eq}} \mathbf{U}_c^* \rangle, \quad (77)$$

$$L_{ci} = L_{ic} = \frac{1}{\xi_c} \langle n_i^{\text{eq}} \mathbf{U}_c^* \rangle. \quad (78)$$

The Hückel limit, for which  $\mathbf{U}_c^* = 0$  in the fluid region, thus corresponds to the case of vanishing hydrodynamic cross-coupling between the colloidal diffusion flux and the thermodynamic forces in the fluid.

To obtain analytical expressions for the auxiliary hydrodynamic tensors, we may consider the dilute limit where the representative volume element  $\mathcal{V}$  consists only of one colloid suspended in a solution, such that  $\nu_m = \nu_c$  and  $N_c = 1$ . Assuming uniform viscosity ( $\eta = \eta^b$ ), the friction tensor of a spherical, homogeneous colloid of hydrodynamic radius  $R$  is given by

$$\boldsymbol{\xi}_c = \xi_c \mathbf{I} = 6\pi s \eta R \mathbf{I}, \quad (79)$$

where the hydrodynamic slip parameter  $s = (1 + 2l_{\text{slip}}/R)/(1 + 3l_{\text{slip}}/R)$  takes the value 1 for a no-slip boundary condition and 2/3 for a perfect-slip boundary condition. To leading order, the backflow required to satisfy Eq. (56) decays with  $1/L$ , where  $L$  is the mesoscopic length scale. By letting the boundaries of  $\mathcal{V}$  tend to infinity from the colloid, the auxiliary hydrodynamic tensors then take the familiar forms for an unbounded solution:

$$\mathbf{U}_c^* = \frac{3R}{4r} \left[ s(\mathbf{I} + \hat{\mathbf{r}}\hat{\mathbf{r}}) - \left( s - \frac{2}{3} \right) \frac{R^2}{r^2} (3\hat{\mathbf{r}}\hat{\mathbf{r}} - \mathbf{I}) \right], \quad (80)$$

$$\boldsymbol{\Lambda}_c^* = -\frac{9\eta R}{2r^2} \left[ s\hat{\mathbf{r}}\hat{\mathbf{r}} - \left( s - \frac{2}{3} \right) \frac{R^2}{r^2} (3\hat{\mathbf{r}}\hat{\mathbf{r}} - \mathbf{I}) \right], \quad (81)$$

where  $r$  is the radial distance from the hydrodynamic centre of the colloid and  $\hat{\mathbf{r}}$  is the outward-pointing radial unit vector. Alternatively, Eq. (81) can be expressed as  $\boldsymbol{\Lambda}_c^* = 9\eta s R \mathbf{I} / (2r^2) - 6\eta \mathbf{U}_c^* / r$ . With Eqs. (79) and (81), the contribution due to microswimming in Eq. (73) then becomes

$$\frac{1}{\xi_c} \cdot \oint_{\partial\nu_c} (\boldsymbol{\Lambda}_c^* \cdot \mathbf{u}_a) dS = -\frac{1}{4\pi R^2} \left( 3 - \frac{2}{s} \right) \oint_{\partial\nu_c} \mathbf{u}_a dS. \quad (82)$$

This expression vanishes for a perfect-slip boundary condition ( $s = 2/3$ ), whereas it reduces to the familiar form  $-1/(4\pi R^2) \oint_{\partial\nu_c} \mathbf{u}_a dS$  for a no-slip boundary condition ( $s = 1$ ), [28] thereby generalising the latter result to arbitrary hydrodynamic slippage at the colloidal surface.

## 6 Continuum-statistical formulation of colloidal diffusion

To obtain a computable continuum-statistical form of the colloidal diffusion flux, we must eliminate from Eq. (73) the thermodynamic forces arising within the solid microphase of the colloids, where the equation of state is usually unknown. To this end, we consider the volume integral of  $\mathcal{F}$  over  $\mathcal{V}$  and write it as a sum of integrals over the colloidal region  $\nu_c$  and fluid region  $\tilde{\nu}$ . Using Eq. (36), this gives

$$\int_{\nu_c} \mathcal{F} d^3\mathbf{r} + \int_{\tilde{\nu}} \mathcal{F} d^3\mathbf{r} = \rho V \mathbf{g} - \int_{\mathcal{V}} \nabla_1 P_s d^3\mathbf{r}, \quad (83)$$

where we have also used the fact that  $\mathcal{V}$  must be overall electroneutral. Based on Eq. (57), the volume integral in Eq. (73) can be written as  $\int_{\mathcal{V}} \mathbf{U}_c^* \cdot \mathcal{F} d^3\mathbf{r} = \int_{\nu_c} \mathcal{F} d^3\mathbf{r} + \int_{\bar{\nu}} \mathbf{U}_c^* \cdot \mathcal{F} d^3\mathbf{r}$ . Using Eq. (83) to eliminate the volume integral over the colloidal region, this becomes

$$\int_{\mathcal{V}} \mathbf{U}_c^* \cdot \mathcal{F} d^3\mathbf{r} = \int_{\bar{\nu}} (\mathbf{U}_c^* - \mathbf{I}) \cdot \mathcal{F} d^3\mathbf{r} + \rho V \mathbf{g} - \int_{\mathcal{V}} \nabla_1 P_s d^3\mathbf{r}. \quad (84)$$

In the fluid region, the thermodynamic force density  $\mathcal{F}$  can now be decomposed into a bulk contribution  $\mathcal{F}^b$  and a disturbance  $\delta\mathcal{F}$  induced by the colloids relative to the bulk fluid, such that  $\mathcal{F} = \delta\mathcal{F} + \mathcal{F}^b$ . At RLTE, the contribution  $\mathcal{F}^b$  is uniform inside a pure bulk solution, whereas it has no statistical correlation with the Stokes flow tensor  $\mathbf{U}_c^*$  inside a homogeneous bulk fluid. Using Eqs. (56) and (57), we can therefore write

$$\int_{\bar{\nu}} (\mathbf{U}_c^* - \mathbf{I}) \cdot \mathcal{F} d^3\mathbf{r} = \int_{\bar{\nu}} (\mathbf{U}_c^* - \mathbf{I}) \cdot \delta\mathcal{F} d^3\mathbf{r} - \int_{\mathcal{V}} \mathcal{F}^b d^3\mathbf{r}. \quad (85)$$

Based on the osmo-mechanical form given by Eq. (38), the induced thermodynamic force density inside the fluid can be expressed as

$$\delta\mathcal{F} = \delta\rho\mathbf{g} + \delta\omega\mathbf{E} + \omega^b\delta\mathbf{E} - \nabla_1\delta\Pi - \nabla_1\delta p. \quad (86)$$

Since the hydrostatic response of the solvent reservoir cannot drive colloidal motion,  $\delta p$  must follow a spherically symmetric decay far away from a colloid in the dilute limit and fulfill a statistical invariance under translation in a homogeneous suspension. From this and Eq. (30), it directly follows that  $\int_{\bar{\nu}} \nabla_1\delta p d^3\mathbf{r} = \oint_{\partial\nu} \delta p \mathbf{n} dS - \oint_{\partial\nu_c} \delta p \mathbf{n} dS = 0$ . Moreover,  $\mathbf{U}_c^* \cdot \nabla_1\delta p = \nabla \cdot (\delta p \mathbf{U}_c^*)$  because  $\nabla \cdot \mathbf{U}_c^* = 0$ . Based on the same arguments, we have  $\int_{\bar{\nu}} \mathbf{U}_c^* \cdot \nabla_1\delta p d^3\mathbf{r} = \oint_{\partial\nu} \delta p \mathbf{U}_c^* \cdot \mathbf{n} dS - \oint_{\partial\nu_c} \delta p \mathbf{U}_c^* \cdot \mathbf{n} dS = 0$ , where we also used Eqs. (30) and (55) and  $\mathbf{U}_c^* \cdot \mathbf{n}|_{\partial\nu_c} = \mathbf{I}$ . Hence,

$$\int_{\bar{\nu}} (\mathbf{U}_c^* - \mathbf{I}) \cdot \nabla_1\delta p d^3\mathbf{r} = 0. \quad (87)$$

Although the bulk fluid is not expected to be electroneutral everywhere within  $\mathcal{V}$  if it contains other species of microparticles ( $\omega^b \neq 0$ ), it must remain overall electroneutral over  $\mathcal{V}$ , such that

$$\int_{\mathcal{V}} \mathcal{F}^b d^3\mathbf{r} = m^b \mathbf{g} - \int_{\mathcal{V}} \nabla_1 P_s^b d^3\mathbf{r}, \quad (88)$$

where  $P_s^b$  is the hydrostatic pressure of the bulk fluid and  $m^b = \int_{\mathcal{V}} \rho^b d^3\mathbf{r}$  is the mass of the bulk fluid inside  $\mathcal{V}$ . As illustrated in Fig. 3, the colloidal osmotic pressure  $\Pi_c$ , which only depends on the osmotic equation of state of the colloids, can now be introduced via

$$\oint_{\partial\nu} \Pi_c \mathbf{n} dS = \int_{\mathcal{V}} \nabla_1 (P_s - P_s^b) d^3\mathbf{r}. \quad (89)$$

Using Eqs. (84)-(89) in Eq. (73), the colloidal diffusion velocity finally takes the continuum-statistical form

$$\begin{aligned} \mathbf{v}_c - \langle \mathbf{u} \rangle = \frac{1}{N_c \xi_c} \cdot & \left[ \int_{\bar{\nu}} (\mathbf{U}_c^* - \mathbf{I}) \cdot (\delta\omega\mathbf{E} + \omega^b\delta\mathbf{E} - \nabla_1\delta\Pi) d^3\mathbf{r} \right. \\ & + \left( m_c - \int_{\nu_c} \rho^b d^3\mathbf{r} + \int_{\bar{\nu}} \delta\rho \mathbf{U}_c^* d^3\mathbf{r} \right) \cdot \mathbf{g} \\ & - \oint_{\partial\nu} \Pi_c \mathbf{n} dS \\ & \left. + \oint_{\partial\nu_m} \boldsymbol{\Lambda}_c^* \cdot \mathbf{u}_a dS \right], \end{aligned} \quad (90)$$

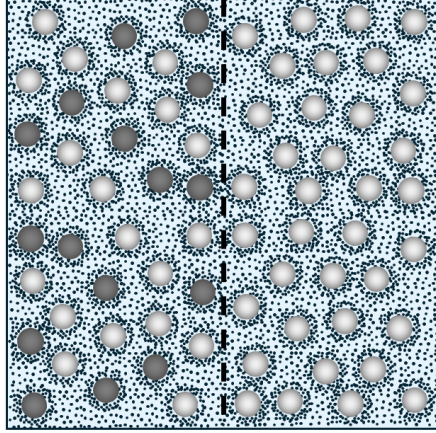


Figure 3: Continuum-mechanically, the osmotic pressure of the colloids (dark spheres) is defined as the pressure difference across a semi-permeable membrane (dashed line) that separates the bulk fluid from the suspension.

where  $m_c$  is the mass of the  $N_c$  colloids inside the representative volume element  $\mathcal{V}$ .

To first order in the non-equilibrium forces, Eq. (90) provides a complete description of colloidal diffusion in a homogeneous suspension and reduces to the diffusion velocity of a single colloid relative to a bulk solution in the dilute limit. Notably, all terms in Eq. (90) have been derived from a single application of the LRT using the auxiliary Stokes flow problem of colloidal sedimentation. The first term represents (self-)phoretic motion, which is consistent with its force-free nature: overall, fluid flows in the direction of the induced phoretic force density  $\mathcal{F}_{\text{ph}} = \delta\omega\mathbf{E} + \omega^b\delta\mathbf{E} - \nabla_1\delta\Pi$ , whereas the colloid is pushed in the opposite direction. The BLA for phoretic motion of a single colloid, applied to thermophoresis by Derjaguin[4] and known as the Smoluchowski limit in electrophoresis, can be recovered from this term by assuming uniform gradients and a no-slip hydrodynamic boundary condition. Using Eq. (80) and expanding the first term to first order in  $z = r - R \ll R$ , one then recovers the well-known BLA expression[6]

$$\int_{\bar{\nu}} (\mathbf{U}_c^* - \mathbf{I}) [\dots] d^3\mathbf{r} = -4\pi R^2 \int_0^\infty z [\dots] dz, \quad (91)$$

where [...] is a placeholder for the corresponding interfacial excess density. The second term in Eq. (90) accounts for buoyant sedimentation, including a hydrodynamic drag caused by the fluid excess weight ( $\delta\rho\mathbf{U}_c^*$ ). The third term consisting of the surface integral over  $\partial\mathcal{V}$  of the colloidal osmotic pressure  $\Pi_c$  accounts for thermal fluctuations and hydrostatic many-body interactions of the colloids.[17] In a homogeneous suspension, this term can also be written as

$$- \oint_{\partial\mathcal{V}} \Pi_c \mathbf{n} dS = -V \bar{\nabla} \Pi_c. \quad (92)$$

If the induced thermodynamic force density  $\delta\mathcal{F}$  is expressed in terms of non-equilibrium thermodynamic disturbances based on Eq. (39), instead of osmo-mechanical disturbances based on Eq. (38), Eq. (90) also aligns with a previously developed Onsager reciprocal treatment.[6] The predictions issuing from this treatment have been verified numerically using mesoscale-molecular simulations,[29] successfully applied to experimental data on thermophoresis of DNA,[30] and used to generalise the Henry function for electrophoresis and the Ruckenstein function for thermophoresis to arbitrary hydrodynamic slippage and interfacial excess

layer thicknesses.[21] However, this Onsager approach simply postulated reciprocal relations, did not account for microswimming or advection, and evaluated the contributions to the colloidal velocity per thermodynamic force without clarifying the role of the solvent reservoir in momentum relaxation. The continuum-statistical framework presented here overcomes these limitations, demonstrating that reciprocity emerges from kinematic reversibility at the continuum scale, encompassing the condition of RLTE. Also note that only the Onsager coefficients  $L_{kq}$  and  $L_{kj}$  of the local solute diffusion fluxes in Eq. (40) remain to be determined. Since the solvent components are at much higher number density than the solute components, one may also adopt a frame of zero mean volume flux for solute diffusion, and hence use Eq. (90) to compute the solute diffusion fluxes, by scaling the continuum approximation down to the molecular scale. In fact, Agar et al. used Onsager symmetry based on the auxiliary Stokes flow around a spherical solute to predict the thermophoresis of ions.[5] Deviations between theoretical predictions and experimental values were explained by limitations in the used Born model of solvation. Another plausible reason for these deviations may be a non-negligible Knudsen number, as small solutes have sizes comparable to water molecules. Although this does not invalidate the form of Eq. (90), a breakdown of LTE is then already expected at weaker gradients. Moreover, the definition of a continuous solid boundary or hydrodynamic radius of a solute particle becomes unphysical at high Knudsen number, suggesting that its friction coefficient may be better described using molecular-dynamical considerations.

## 7 Application to diffusiophoresis due to volume exclusion of a solute

To apply our results, we focus on colloidal diffusion in the dilute limit, where analytical expressions of colloidal mobilities can be obtained based on a known osmotic equation of state of the fluid. A well-known example is that of a Poisson-Boltzmann-Born (PBB) solution, given by

$$\Pi = k_B T \sum_k n_k + \frac{1}{2} \epsilon (\nabla \varphi)^2, \quad (93)$$

$$n_k = n_k^r \exp\left(-\frac{\phi_k}{k_B T}\right). \quad (94)$$

The first term in Eq. (93) accounts for the ideal osmotic pressure of the solutes, whereas the second term represents the electrostatic field energy density, which yields the Born free energy of solvation when polarisable solvent molecules interact with the electrostatic potential  $\varphi$  of a charged colloid.[5] Under non-equilibrium boundary conditions, the second term gives rise to an effect known as electrostriction,[1] which is relevant for the thermophoresis of charged colloids in aqueous electrolyte solutions.[20]

In particular, our framework predicts a novel contribution to phoretic motion that does not derive from interfacial excess, but from thermodynamic force disturbances, as discussed in the context of Eq. (33). In general, such disturbances display a slower decay with distance than those due to interfacial excess and can therefore not be considered in the BLA. This might be the reason why the contribution has been claimed to be absent elsewhere,[15] based on the assumption that the solvent reservoir can balance such long-range disturbances. However, according to Eq. (33), our framework suggests that these disturbances should be treated on an equal footing with those induced by interfacial excess, thus producing a convergent contribution to the colloidal diffusion velocity.

To evidence this, we consider the diffusiophoretic motion at constant temperature of a single colloid whose solid boundary is defined by its hydrodynamic radius  $R$ . The colloid is suspended in a PBB solution

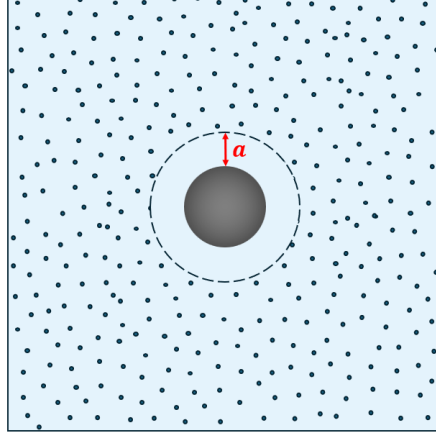


Figure 4: The excluded volume interaction between the colloid and the solute leads to an interfacial excess layer around the colloid that is completely void of solute particles.

composed of a solvent and a single ideal solute component, whose index  $k$  can thus simply be omitted. We assume that the colloid only interacts with the solute via an excluded volume potential  $\phi = \infty$  within a range  $r \leq R + \lambda$ , where  $\lambda$  is the thickness of the excluded volume layer around the solid boundary of the colloid. The osmotic equation of state of the fluid is hence given by

$$\Pi = nk_B T, \quad (95)$$

where  $n$  is the number density of the solute. Diffusiophoresis is caused by a gradient in solute number density across  $\mathcal{V}$ , which produces an osmotic pressure gradient that tends to a uniform bulk value  $\nabla_1 \Pi^b = k_B T \nabla n^b$  far away from the colloidal surface. From Eqs. (40) and (41), or equivalently Eq. (90), it follows that the diffusion flux of an ideal solute reservoir must reduce to the diagonal form  $\mathbf{j} = -1/\xi \nabla_1 \Pi = -n^{\text{eq}}/\xi \nabla_T \mu$ , where  $\xi$  is the friction coefficient of a solute particle and  $\nabla_T \mu = k_B T \nabla n^r / n^{b \text{eq}}$ . Using Eq. (94), we can thus write

$$\mathbf{j} = -D \nabla n^r, \quad (96)$$

$$D = \frac{k_B T}{\xi} \exp\left(-\frac{\phi}{k_B T}\right). \quad (97)$$

The effective diffusion coefficient  $D$  of the solute reservoir is uniform for  $r > R + \lambda$  but zero for  $r \leq R + \lambda$ , which corresponds to a condition of zero normal solute diffusion flux  $\nabla n^r \cdot \hat{\mathbf{r}} = 0$  at  $r = R + \lambda$ . As a result, we also have  $n^r = 0$  and  $\nabla n^r = 0$  for  $r \leq R + \lambda$ , so that the interfacial excess number density  $-n^b$  of the solute cannot couple to a corresponding gradient inside the excluded volume layer. The osmotic pressure gradient in the fluid therefore takes the form  $\nabla_1 \Pi = n^b \nabla_T \mu = k_B T \nabla n^r$ , implying that  $\nabla_1 \delta \Pi$  exclusively stems from a disturbance in the thermodynamic force  $\nabla_T \mu$ . We can hence write

$$\nabla_1 \delta \Pi = k_B T \left[ -\chi_{]R, R+\lambda]} \nabla n^b + n^r \delta_{R+\lambda} \hat{\mathbf{r}} + \chi_{]R+\lambda, \infty[} \nabla (n^r - n^b) \right], \quad (98)$$

where  $\delta_{R+\lambda}$  is the delta distribution supported at  $r = R + \lambda$  and where the indicator function  $\chi$  is equal to unity within the specified range of  $r$  and zero otherwise. In Eq. (98), the first term represents the disturbance

of  $\nabla n^r$  inside the excluded volume layer. Although different in nature, this term coincides with the term obtained when the interfacial excess number density  $-n^b$  is assumed to couple to the bulk gradient  $k_B T \nabla n^b$ , corresponding to the familiar treatment of phoretic motion under uniform gradients. Consequently, this term must yield the diffusiophoretic velocity as derived by Anderson when the BLA is applied under a no-slip hydrodynamic boundary condition at the colloidal surface.[7] The second term is a singular contribution due to the jump of  $\nabla_1 \delta \Pi$  from  $-n^b k_B T$  to  $(n^r - n^b) k_B T$  when passing from  $r \leq R + \lambda$  to  $r > R + \lambda$ . Lastly, the third term stems from the diffusive polarisation of solute around the excluded volume layer due to the condition of zero normal diffusion flux at  $r = R + \lambda$ . Our aim is to derive an explicit expression for the colloidal diffusion velocity in terms of the bulk gradient  $\nabla n^b$ , such that

$$\mathbf{v}_c - \langle \mathbf{u} \rangle = -\frac{R^2}{9\eta} M k_B T \nabla n^b, \quad (99)$$

where  $M$  is the rescaled diffusiophoretic mobility of the colloid. In the absence of gravity and microswimming, Eq. (90) reduces to

$$\mathbf{v}_c - \langle \mathbf{u} \rangle = -\frac{1}{\xi_c} \int_{\tilde{v}} (\mathbf{U}_c^* - \mathbf{I}) \cdot \nabla_1 \delta \Pi d^3 \mathbf{r}. \quad (100)$$

Solving the continuity equation  $\nabla \cdot \mathbf{j} = 0$  for the solute particles to express  $\nabla_1 \delta \Pi$  in terms of the bulk gradient  $\nabla n^b$  only, Eq. (98) yields

$$\nabla_1 \delta \Pi = n^{\text{bleq}} \delta_{R+\lambda} \hat{\mathbf{r}} + \left[ -\chi_{]R, R+\lambda]} \mathbf{I} + \frac{3}{2} (R + \lambda) \delta_{R+\lambda} \hat{\mathbf{r}} \hat{\mathbf{r}} - \frac{1}{2} \chi_{]R+\lambda, \infty[} \frac{(R + \lambda)^3}{r^3} (3\hat{\mathbf{r}} \hat{\mathbf{r}} - \mathbf{I}) \right] \cdot k_B T \nabla n^b. \quad (101)$$

Using Eqs. (79), (80) and (101) in Eq. (100), and introducing the dimensionless interfacial width parameter  $x = \lambda/R$ , the diffusiophoretic mobility in Eq. (99) finally takes the form

$$M = \underbrace{\frac{x}{s} [2x^2 - 3(s-2)x - 6(s-1)]}_{M_{]R, R+\lambda]}} + \underbrace{\frac{3}{s} \left[ (1+x)^3 - \frac{3}{2}s(1+x)^2 + \frac{3}{2}s - 1 \right]}_{M_{R+\lambda}} \underbrace{-\frac{1}{s}(1+x)^3}_{M_{]R+\lambda, \infty[}}, \quad (102)$$

which is equivalent to Eq. (1), but distinguishes the contributions to  $M$  from different intervals of  $r$ .

If only the contribution  $M_{]R, R+\lambda]}$  from within the excluded volume layer is taken into account, then imposing a no-slip boundary condition ( $s = 1$ ) and expanding this term to leading order in  $x \ll 1$  gives  $M = 3x^2$ . Using this in Eq. (100), we obtain

$$\mathbf{v}_c - \langle \mathbf{u} \rangle = -\frac{\lambda^2}{3\eta} k_B T \nabla n^b. \quad (103)$$

Based on the relation between the colloidal diffusion velocity and the surface-averaged diffusio-osmotic slip velocity obtained in the BLA, Eq. (103) indeed coincides with the result derived by Anderson,[7] which assumes that the interfacial excess density  $-n^b$  couples to a uniform bulk gradient within the layer. Hence, Eq. (102) generalises this result to arbitrary layer thickness  $\lambda$  and hydrodynamic slippage  $s$  at the colloidal surface, while also accounting for the contribution  $M_{R+\lambda}$  from the outer boundary of the layer and the contribution  $M_{]R+\lambda, \infty[}$  from the diffusive polarisation of solute outside the layer. Due to the latter two contributions, the diffusiophoretic mobility  $M$  predicted by Eq. (102) differs considerably from Eq. (103). This is shown in Fig. 5, where  $M$  is plotted as a function of  $x = \lambda/R$  for three different values of the hydrodynamic slip parameter  $s$ . Whereas Anderson's result exclusively predicts diffusiophoresis towards

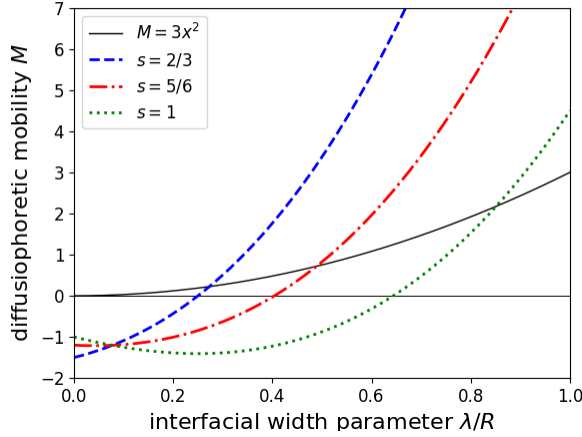


Figure 5: Rescaled diffusiophoretic mobility  $M$  of a single colloid due to volume exclusion of an ideal solute, plotted against the interfacial width parameter  $x = \lambda/R$  for three different values of the hydrodynamic slip parameter  $s$ . The BLA applies for  $x \ll 1$ , whereas the Hückel limit applies for  $x \gg 1$ . The excluded volume layer is usually thin compared to the colloidal radius, implying that the BLA is often the more realistic limit for diffusiophoresis.

lower bulk solute concentration ( $M = 3x^2 \geq 0$ ), Eq. (102) predicts the opposite trend ( $M < 0$ ) over the entire range of hydrodynamic slippage  $2/3 \leq s \leq 1$  in the BLA ( $x \ll 1$ ), while a crossover towards positive values of  $M$  eventually occurs at  $x = 0.25$  for perfect slip ( $s = 2/3$ ) and at  $x \approx 0.64$  for no slip ( $s = 1$ ). In particular, only the diffusive polarisation term  $M_{]R+\lambda, \infty]}$  persists when the excluded volume layer is removed by setting  $x = 0$ . In this case,  $M = -1/s$  and Eq. (99) reduces to

$$\mathbf{v}_c - \langle \mathbf{u} \rangle = \frac{R^2}{9s\eta} k_B T \nabla n^b. \quad (104)$$

Eq. (104) shows that diffusiophoresis occurs even in the absence of an interfacial potential interaction and predicts motion towards higher bulk solute concentration, as shown in Fig. 6a), with speeds of  $\sim 0.1 - 1 \mu\text{m/s}$  based on typical parameter values. This behavior can be understood intuitively: As the solute cannot diffuse through the colloid, it accumulates on the side of the colloid facing the bulk solute flux and depletes from the other side. The induced osmotic pressure gradient then drives a local fluid flow towards lower bulk solute concentration, thus pulling the colloid in the opposite direction. Under the same bulk gradient  $\nabla n^b$ , one may alternatively consider an active colloid with a perfectly absorbing surface, such that the boundary condition for solute diffusion changes from  $\nabla n^r \cdot \hat{\mathbf{r}} = 0$  to  $n^r = 0$  at the colloidal surface, as shown in Fig. 6b). In this case, one obtains  $\nabla_1 \delta \Pi = \chi_{[R, \infty]} R^3 / r^3 (3\hat{\mathbf{r}}\hat{\mathbf{r}} - \mathbf{I}) \cdot k_B T \nabla n^b$ , which instead produces a colloidal velocity

$$\mathbf{v}_c - \langle \mathbf{u} \rangle = -\frac{2R^2}{9s\eta} k_B T \nabla n^b, \quad (105)$$

corresponding to colloidal motion towards lower bulk solute concentration. This example demonstrates that phoretic motion is not only highly sensitive to interfacial potential interactions, but also to interfacial boundary conditions, whose variations can reverse the direction of colloidal motion under identical bulk conditions.

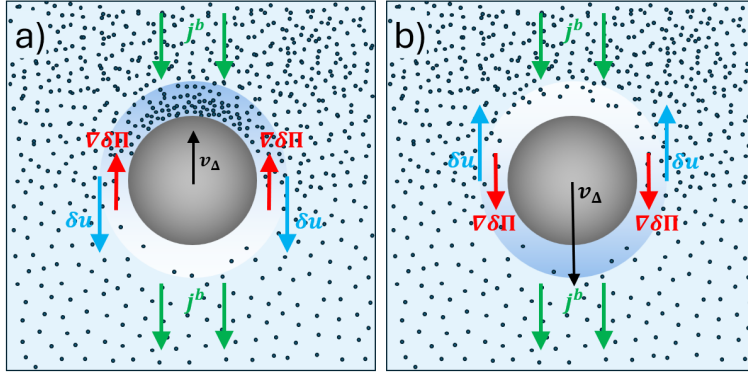


Figure 6: Diffusiophoresis of a single colloid caused by a disturbance of the number density gradient  $\nabla n^r$  of the solute reservoir, in the absence of an interfacial potential interaction. a) Diffusive polarisation across a passive colloid, resulting in a diffusiophoretic velocity given by Eq. (104). b) An active colloid with a perfectly absorbing surface, producing a diffusiophoretic velocity given by Eq. (105). The green arrows show the direction of the bulk solute flux  $\mathbf{j}^b$ , the red arrows the direction of the induced osmotic pressure gradient  $\nabla_1 \delta \Pi$ , the blue arrows the direction of the induced average fluid flow, and the black arrows the resulting diffusion velocity  $\mathbf{v}_\Delta = \mathbf{v}_c - \langle \mathbf{u} \rangle$  of the colloid. The color gradient around the colloidal surface is a schematic representation of  $\delta \Pi$ , with low values in white and high values in dark blue.

## 8 Conclusion

In general, resolving the local continuum dynamics in colloidal suspensions is both theoretically and computationally demanding, as it requires solving multiple coupled continuity equations under moving boundary conditions. As a result, many existing approaches rely on linear-response models that treat diffusive transport, including force-free phoretic motion, in a largely phenomenological manner.

Here, we have shown that reducing this phenomenology does not require explicit resolution of the full microhydrodynamics, by formulating colloidal motion within a continuum-statistical framework grounded in kinematic reversibility. In this formulation, Onsager reciprocal relations arise naturally from the symmetry of the hydrodynamic response encoded in the Lorentz reciprocal theorem. Our framework consistently accounts for the solvent reservoir response to momentum relaxation and fully resolves the coupling between thermodynamic forces and hydrodynamic flows beyond the boundary layer approximation. As summarised for a single colloid in Fig. 7, our approach decomposes into three independent and computationally tractable parts that represent the essential physical ingredients of a reciprocal treatment of colloidal motion: an equilibrium-statistical problem to determine osmotic equations of state and local component distributions (Fig. 7b)), a hydrodynamic problem to compute the auxiliary Stokes flow under stationary boundary conditions (Fig. 7d)), and a steady-state problem to determine the local thermodynamic forces (Fig. 7c)). The underlying linear-response assumption is not unduly restrictive, as fluxes are almost universally taken to be linear in the non-equilibrium forces in advection–diffusion problems. Applying this approach beyond the dilute limit to dense suspensions, by numerically solving the full set of mesoscopic continuity equations, represents a natural and promising direction for future work.

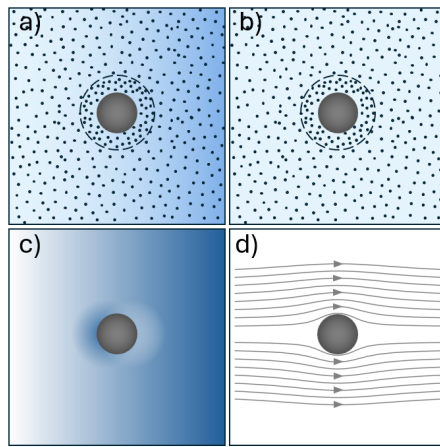


Figure 7: Schematic representation of the reciprocal approach to colloidal motion. a) A single colloid subjected to non-equilibrium forces. The continuum fields that these forces derive from are illustrated by a blue background gradient. The dashed circle around the colloid represents the effective boundary between its interfacial region and the bulk fluid. Instead of resolving the full local dynamics of a), the reciprocal approach consists of three alternative parts: b) An equilibrium-statistical problem to determine local component distributions, and a continuum-mechanical problem to independently compute c) the non-equilibrium forces and d) the induced Stokes flow field. A stronger background gradient is used in c) to show that the colloid can modify the continuum fields in its vicinity if the transport properties of its solid microphase differ from those of the solution.

## A Derivation of the mesoscopic continuity equations

Since interfacial potential interactions can only redistribute component particles within a solid microphase, the partial volume averages of the component number densities of a given solid microphase  $\alpha$  satisfy  $\langle n_i \rangle_{\nu_\alpha} = \langle n_i^r \rangle_{\nu_\alpha}$ . To introduce the colloids as a mesoscopic component of the suspension, we can therefore write the number of constituent component particles per colloid as  $\mathcal{N}_c = V \sum_j \langle n_j^r \rangle / N_c$ , where the index  $j$  runs over all components that are part of the solid microphase of the colloids. We further assume that the composition of a colloid remains largely insensitive to chemical reactions on its surface, such that  $\mathcal{N}_c$  remains constant. We can then introduce the number density of the colloidal component as  $n_c = \sum_j \langle n_j^r \rangle / N_c$  and the corresponding particle flux as  $\mathbf{J}_c = \sum_j \langle \mathbf{J}_j \rangle / N_c$ , and separately introduce a colloidal chemical source density  $\Gamma_c$  at the mesoscopic scale. With Eqs. (16) and (20), the continuity equation of the colloidal component thus becomes

$$\frac{\partial n_c}{\partial t} + \bar{\nabla} \cdot \mathbf{J}_c = \Gamma_c, \quad (106)$$

where the colloidal flux  $\mathbf{J}_c$  can be written as

$$\mathbf{J}_c = n_c \langle \mathbf{u} \rangle + \mathcal{J}_c. \quad (107)$$

Substituting Eq. (107) into Eq. (106) and using Eq. (19), the colloidal continuity equation can hence also be rewritten as

$$\frac{\partial n_c}{\partial t} + \langle \mathbf{u} \rangle \cdot \bar{\nabla} n_c + \bar{\nabla} \cdot \mathcal{J}_c = \Gamma_c, \quad (108)$$

which recovers Eq. (23). The constituent particles of a colloid are chemically bound and therefore cannot undergo local diffusion ( $\mathbf{j}_c = 0$ ). Based on Eq. (22), the diffusion flux  $\mathcal{J}_c$  of the colloids is therefore a pure diffusion flow, such that  $\mathcal{J}_c = \langle n_c \mathbf{u}' \rangle = n_c \langle \mathbf{u}' \rangle_{\nu_c}$ , where  $\langle \mathbf{u}' \rangle_{\nu_c} = \langle \mathbf{u} \rangle_{\nu_c} - \langle \mathbf{u} \rangle$  is the diffusion velocity of the colloids. To relate the mean diffusion flow of a component  $i$  of the solution ( $i \in \nu_\eta$ ) to the colloidal diffusion fluxes, we use Eqs. (18) and (8) to obtain

$$\langle n_i^r \mathbf{u}' \rangle = -\gamma_m \langle n_i^{r|\text{eq}} \rangle_{\nu_\eta} \langle \mathbf{u}' \rangle_{\nu_m}, \quad (109)$$

to first order in the non-equilibrium forces, where  $\gamma_m = V_m/V$  is the microparticle volume fraction. Note that no volume averaging over  $\nu_\eta$  is required for  $\langle n_i^{r|\text{eq}} \rangle_{\nu_\eta}$  because  $n_i^{r|\text{eq}}$  is uniform inside  $\nu_\eta$ . Moreover, we can relate the mean diffusion flow velocity of the microparticles to the colloidal diffusion fluxes via

$$\langle \mathbf{u}' \rangle_{\nu_m} = \frac{V}{\sum_c N_c} \sum_c \mathcal{J}_c. \quad (110)$$

Upon substitution of Eq. (110) into Eq. (109), the mean diffusion flow of a component of the solution in terms of the colloidal diffusion fluxes becomes

$$\langle n_i^r \mathbf{u}' \rangle = -\bar{V}_m \langle n_i^{r|\text{eq}} \rangle_{\nu_\eta} \sum_c \mathcal{J}_c, \quad (111)$$

where  $\bar{V}_m = V_m / \sum_c N_c$  is the average volume of a microparticle inside  $\mathcal{V}$ . Using Eq. (111) in Eq. (22), followed by a substitution of Eq. (21) into Eq. (16), the mesoscopic continuity equation of a solute or solvent component thus takes the form

$$\frac{\partial \langle n_i^r \rangle}{\partial t} + \langle \mathbf{u} \rangle \cdot \bar{\nabla} \langle n_i^r \rangle - \bar{\nabla} \cdot \left( \bar{V}_m \langle n_i^{r|\text{eq}} \rangle_{\nu_\eta} \sum_c \mathcal{J}_c \right) + \bar{\nabla} \cdot \langle \mathbf{j}_i \rangle = \langle \Gamma_i \rangle. \quad (112)$$

This continuity equation describes the evolution of the volume-averaged reservoir number densities that set the boundary conditions on a given volume element to determine the local steady-state distributions inside the solution.

Averaging the local momentum continuity equation, as given by Eq. (10), over a volume element  $\mathcal{V}$ , and using Eq. (6), we obtain

$$\langle \mathbf{f} \rangle + \bar{\nabla} \cdot \langle \boldsymbol{\sigma} \rangle = 0. \quad (113)$$

For a homogeneous suspension at RLTE, the condition of mesoscopic electroneutrality implies that only gravitational forces contribute to the net body force acting on  $\mathcal{V}$ , such that

$$\langle \mathbf{f} \rangle = \langle \rho \rangle \mathbf{g}. \quad (114)$$

The suspension stress tensor  $\langle \boldsymbol{\sigma} \rangle$  can be decomposed into a scalar contribution and a shear stress. Using an overbar to denote mesoscopic suspension properties, we can therefore write

$$\langle \boldsymbol{\sigma} \rangle = -\bar{P} \mathbf{I} + \bar{\boldsymbol{\Sigma}}, \quad (115)$$

where  $\bar{P}$  is the suspension pressure and  $\bar{\boldsymbol{\Sigma}}$  is the suspension shear stress tensor. The shear stress tensor of an incompressible, isotropic suspension must have a purely viscous form, such that  $\bar{\boldsymbol{\Sigma}} = \bar{\eta} \langle \mathbf{e} \rangle$ , where  $\langle \mathbf{e} \rangle = (\bar{\nabla} \langle \mathbf{u} \rangle + \bar{\nabla}^\dagger \langle \mathbf{u} \rangle) / 2$  is the strain rate tensor of the advective velocity  $\langle \mathbf{u} \rangle$ , and  $\bar{\eta}$  is the dynamic viscosity of the suspension, which can be determined from hydrodynamic considerations.[31] The suspension pressure can further be decomposed into a hydrostatic pressure  $\bar{P}_s$ , and a hydrodynamic pressure  $\bar{P}_d$  that vanishes in the absence of advection:

$$\bar{P} = \bar{P}_s + \bar{P}_d, \quad (116)$$

where

$$\bar{\nabla} \bar{P}_s = \langle \nabla_1 P_s \rangle = \langle \nabla_1 \Pi \rangle + \langle \nabla_1 p \rangle. \quad (117)$$

We can now introduce the osmotic pressure  $\bar{\Pi}$  of the suspension as

$$\bar{P}_s = \bar{\Pi} + \bar{p}, \quad (118)$$

where

$$\bar{p} = \langle p \rangle_{\nu_\eta} \quad (119)$$

is the solution-averaged hydrostatic pressure of the solvent reservoir, defined over the entire volume element. Since the hydrostatic solvent reservoir pressure  $p$  is only nonzero inside the solution, we can use Eqs. (6) and (8) to write

$$\langle \nabla_1 p \rangle = (1 - \gamma_m) \bar{\nabla} \bar{p}, \quad (120)$$

also giving  $\bar{\nabla} \bar{\Pi} = \langle \nabla_1 \Pi \rangle - \gamma_m \bar{\nabla} \bar{p}$ . Using Eqs. (114)-(120), the mesoscopic momentum continuity equation thus takes the form

$$\langle \rho \rangle \mathbf{g} - \langle \nabla_1 \Pi \rangle - (1 - \gamma_m) \bar{\nabla} \bar{p} + \bar{\nabla} \cdot \langle \boldsymbol{\sigma}_d \rangle = 0, \quad (121)$$

showing that the volume-averaged gravitational force density and osmotic pressure gradient act as driving forces of advection inside the suspension. With Eqs. (121), we have derived the form of the mesoscopic momentum continuity equation given by Eq. (44).

## References

- [1] Sybren Ruurds De Groot and Peter Mazur. *Non-equilibrium thermodynamics*. Courier Corporation, 2013.
- [2] Lars Onsager. Reciprocal relations in irreversible processes. i. *Physical review*, 37(4):405, 1931.
- [3] Lars Onsager. Reciprocal relations in irreversible processes. ii. *Physical review*, 38(12):2265, 1931.
- [4] Nikolai V Churaev, Boris V Derjaguin, and Vladimir M Muller. *Surface forces*. Springer Science & Business Media, 2013.
- [5] J.N. Agar, Chung-Yuan Mou, and Jeong-Long Lin. Single-ion heat of transport in electrolyte solutions: a hydrodynamic theory. *The Journal of Physical Chemistry*, 93(5):2079–2082, 1989.
- [6] Jérôme Burelbach, Daan Frenkel, Ignacio Pagonabarraga, and Erika Eiser. A unified description of colloidal thermophoresis. *The European Physical Journal E*, 41(1):7, 2018.
- [7] John L Anderson. Colloid transport by interfacial forces. *Annual review of fluid mechanics*, 21(1):61–99, 1989.
- [8] Hassan Masoud and Howard A Stone. A reciprocal theorem for marangoni propulsion. *Journal of Fluid Mechanics*, 741:R4, 2014.
- [9] Jérôme Burelbach and Holger Stark. Linear and angular motion of self-diffusiophoretic janus particles. *Physical Review E*, 100(4):042612, 2019.
- [10] Max Teubner. The motion of charged colloidal particles in electric fields. *The Journal of Chemical Physics*, 76(11):5564–5573, 1982.
- [11] Thomas A Witten and Aaron Mowitz. Adapting the teubner reciprocal relations for stokeslet objects. *arXiv preprint arXiv:1907.07444*, 2019.
- [12] John F Brady. Phoretic motion in active matter. *Journal of Fluid Mechanics*, 922:A10, 2021.
- [13] Arkava Ganguly, Souradeep Roychowdhury, and Ankur Gupta. Unified mobility expressions for externally driven and self-phoretic propulsion of particles. *Journal of Fluid Mechanics*, 994:A2, 2024.
- [14] GK Batchelor. Brownian diffusion of particles with hydrodynamic interaction. *Journal of Fluid Mechanics*, 74(1):1–29, 1976.
- [15] John F Brady. Particle motion driven by solute gradients with application to autonomous motion: continuum and colloidal perspectives. *Journal of Fluid Mechanics*, 667:216–259, 2011.
- [16] John Happel and Howard Brenner. *Low Reynolds number hydrodynamics: with special applications to particulate media*, volume 1. Springer Science & Business Media, 2012.
- [17] Jan KG Dhont. Thermodiffusion of interacting colloids. i. a statistical thermodynamics approach. *The Journal of chemical physics*, 120(3):1632–1641, 2004.
- [18] Jeroen Rodenburg, Marjolein Dijkstra, and René van Roij. Van’t hoff’s law for active suspensions: the role of the solvent chemical potential. *Soft matter*, 13(47):8957–8963, 2017.

- [19] Signe Kjelstrup and Dick Bedeaux. *Non-equilibrium thermodynamics of heterogeneous systems*. World Scientific, 2008.
- [20] Alois Würger. Thermal non-equilibrium transport in colloids. *Reports on Progress in Physics*, 73(12):126601, 2010.
- [21] Jérôme Burelbach. Particle motion driven by non-uniform thermodynamic forces. *The Journal of chemical physics*, 150(14), 2019.
- [22] Hendrik Antoon Lorentz. Attempt of a theory of electrical and optical phenomena in moving bodies. *Versuch einer Theorie der Elektrischen und Optischen Erscheinungen in Bewegten Körpern*. EJ Brill, 1895.
- [23] James R. Bielenberg and Howard Brenner. A continuum model of thermal transpiration. *Journal of Fluid Mechanics*, 546:1 – 23, 2005.
- [24] D Bedeaux, AM Albano, and P Mazur. Boundary conditions and non-equilibrium thermodynamics. *Physica A: Statistical Mechanics and its Applications*, 82(3):438–462, 1976.
- [25] Michael James Lighthill. On the squirming motion of nearly spherical deformable bodies through liquids at very small reynolds numbers. *Communications on pure and applied mathematics*, 5(2):109–118, 1952.
- [26] John R Blake. A spherical envelope approach to ciliary propulsion. *Journal of Fluid Mechanics*, 46(1):199–208, 1971.
- [27] GK Batchelor. The stress system in a suspension of force-free particles. *Journal of fluid mechanics*, 41(3):545–570, 1970.
- [28] Howard A Stone and Aravinthan DT Samuel. Propulsion of microorganisms by surface distortions. *Physical review letters*, 77(19):4102, 1996.
- [29] Jérôme Burelbach, David B. Brückner, Daan Frenkel, and Erika Eiser. Thermophoretic forces on a mesoscopic scale. *Soft matter*, 14 36:7446–7454, 2018.
- [30] Jérôme Burelbach and Holger Stark. Determining phoretic mobilities with onsager’s reciprocal relations: Electro- and thermophoresis revisited. *The European Physical Journal E*, 42, 2018.
- [31] Howard Brenner. Rheology of a dilute suspension of axisymmetric brownian particles. *International journal of multiphase flow*, 1(2):195–341, 1974.